Wireless Transfer of Energy Alongside Information in Wireless Sensor Networks

Hooman Javaheri and Guevara Noubir

Abstract Despite steady improvements over the last few decades, wireless communication networks are still severely constrained by the availability of an energy source. The problem manifests itself in many applications, in particular, wireless sensor networks enabling a plethora of Internet of Things devices, where communications are infrequent and the nodes are often idle; and also small-scale communication networks, whose nodes need to be minuscule limiting the possibilities to incorporate long-term energy peripherals such as batteries. Such applications can achieve optimal energy efficiency using passive (battery-less) receivers that wirelessly receive energy and information at the same time. In this chapter, we describe a set of techniques, introduced in our past work (Javaheri H Wireless Transfer of Energy Alongside Information: From Wireless Sensor Networks to Bio-Enabled Wireless Networks 2012 [37]), (Javaheri, Noubir, ipoint: A platform-independent passive information kiosk for cell phones 2010 [42]), to simultaneously deliver energy alongside information during wireless communications. We present mechanisms to consolidate energy and information transfer in wireless sensor networks. We introduce iPoint, a communication system including a passively powered wireless receiver capable of establishing two-way communication with a commodity smartphone without any hardware modifications. In contrast to traditional RFID tags, iPoint provides high computation and sensing capabilities and most importantly, it does not require specialized reader device to communicate. We prototype and experimentally evaluate our design that includes optimization techniques to ensure efficient delivery of energy and information and novel communication protocols.

H. Javaheri (✉) · G. Noubir
College of Computer and Information Science, Northeastern University,
Boston, MA 02115, USA
e-mail: hooman@ccs.neu.edu

G. Noubir
e-mail: noubir@ccs.neu.edu

H. M. Ammari (ed.), *Mission-Oriented Sensor Networks and Systems: Art and Science*, Studies in Systems, Decision and Control 164,
https://doi.org/10.1007/978-3-319-92384-0_13

1 Introduction

Communication means imparting or exchanging of information among several parties. One important point, which is often overlooked, is that the parties engaged in any form of communication requires a certain amount of energy to send, receive, and process the traveling information. A dead node in a network never receives the message intended for it much like a dead person who will never hear a cry.

Over the last decade, wireless communication networks have achieved major success and emerged as the key technology for enabling the mobile revolution. Providing mobility and accessibility, wireless communication redefines the notion of network and connectivity, and powers a huge range of applications. The speed, capacity and robustness of wireless communication keep improving every day, but several challenges, most notably energy efficiency, hinder their effectiveness [22, 46]. Conserving energy in wireless networks is particularly important because the wireless nodes are critically dependent on their limited energy resource, that is, their battery. Receiving and decoding a wireless signal normally requires a significant amount of computations. In addition, transmitting wireless messages is one of the most energy consuming tasks in today's computing. Performing such energy-hungry tasks with low efficiency reduces the lifetime of the nodes and eventually causes node death degrading connectivity and performance of the network. These challenges are specially critical for the emerging IoT revolution powered by wireless sensor networks. Therefore, several attempts at hardware and software levels have been made to tackle this problem: more efficient batteries with larger capacities have been invented [54]; the power consumption of wireless nodes has been significantly reduced thanks to advances in low-power electronics and new methods of computation such as reversible computing [6]; finally, many energy-aware communication protocols and algorithms that factor in the energy constraints of wireless nodes have emerged [17, 74, 80, 81].

All wireless networks struggle with the energy conservation issue, yet the problem is more evident in certain applications such as wireless sensor networks (WSNs). A WSN usually consists of several spatially distributed nodes that monitor or sense a physical or environmental condition, and transmit the collected data via wireless communication. The sensing process generally does not require a lot of energy. In fact, wireless transmission accounts for almost all the node's energy consumption. In most cases, the data collection occurs sporadically or upon an external request. Therefore, continuous operation of a node's radio, which results in fast battery drainage, is not necessary. Current techniques rely on periodically waking the receiver up to synchronize and respond to the requests of a master node [13, 91]. These methods help conserve energy but are far from optimal. Ideally, the radio component of the sensor node should go into a full-sleep (idle) mode that consumes virtually no energy and wakes up only on external requests or events. This can be achieved by integrating

a completely passive component that acts as a wake-up circuit and relays the external request to the idle node. The challenge of engineering such a system, which includes software, hardware, and communication protocols, is one of the goals of this study.

Having a receiver that consumes *no energy* while being idle is the optimal solution for any of the scenarios mentioned above. Note that, this goal can not be achieved by simply reducing the energy consumption of the radio components; rather, the energy consumption should be eliminated when no communication is taking place. This rules out the use of conventional wireless devices which are basically an ensemble of active electronic boards that consume energy while operating, regardless of how energy-efficient they are. Instead, let us consider the following scenario: assume that the incoming signal, which carries a certain amount of information, provides the receiver with the energy required to extract the information. On the other end, the receiver simultaneously executes two actions on the signal. First, it converts the energy of the signal into a usable form. Second, it runs the decoding procedure to extract the embedded information. In this case, the energy consumption occurs only when there is an incoming signal, and it is fully provided by the transmitter entity. Therefore, the receiver does not rely on any other source of energy.

Combining energy and information transfer is a promising approach that leads to engineering *passive* wireless receivers. There are many communication schemes that provides a vast range of throughput, complexity, and energy efficiency. Also, a few mechanisms such as RF energy harvesting have been proposed to transfer energy wirelessly [53, 86]. However, combining these schemes presents several challenges. The range and capacity of today's energy transfer methods are very limited, which makes pairing them with normal communication methods difficult and often impossible. In order to have a functional system, we need to carefully optimize, modify, or completely revamp the energy and information transfer mechanisms. This includes building more efficient systems using specialized hardware, and devising better algorithms software solutions that exhaust the physical limits of the hardware.

In this chapter, we aim to explore several techniques to transfer energy alongside information via a wireless link. We look into techniques to consolidate the energy and information transfer in wireless networks. We review and compare the energy transfer technologies, provide design considerations, and sketch guidelines to implement such functionality. At the end, we present a communication system that allows two-way communication between a commodity smartphone and a passive receiver. The system features a combination of ultra-low-power electronics and RF energy harvesting. We introduce several techniques to increase the efficiency of the information and energy channels, propose novel communication paradigms and protocols optimized for our setup, build prototypes and finally, evaluate the system performance experimentally.

The contents of this chapter is based on authors' previous work [37, 42]. The results, discussions, and figures may have appeared in other manuscripts published by the authors.

Chapter Organization The rest of this chapter is structured as follows:
In Sect. 3, we define a model for consolidated energy and information channels in wireless sensor network. We describe the framework for our model and review the

building blocks of such model along with its design requirements. This section serves as the basis for Sect. 4 in which we present iPoint.

Section 4 includes a comprehensive design, optimization, prototype, and performance evaluation of iPoint, a novel communication system that features a consolidated energy and information channel. This includes the design and characterization of hardware, software, and communication paradigms. Several optimization techniques including theoretical analysis and experimental validations are detailed. A shorter version of the results presented in this section has been published in [42].

Section 2 reviews the related literature. We discuss previous studies in the field, which presents the state-of-the-art for relevant technologies and identify the similarities and distinctions of our work. Section 5 concludes the document and presents the direction for future work.

2 Related Work

2.1 Radio Frequency Identification (RFID)

RFID tags have the potential to deliver information anytime, anywhere [23, 88]. However, RFID tags have significant limitations making them impractical for delivering a substantial amount of information to commodity smartphones. First of all, equipping smartphones with an RFID reader is a significant and challenging modification to the phone hardware. Second, among the three types of RFIDs (i.e., passive, active, and semi-active), only the passive ones do not require a battery and therefore satisfy severe longevity constraints. However, passive RFIDs require the readers to transmit at high power (in the order of watts), with large antennas. Furthermore, such RFIDs are only capable of storing a very limited amount of information (e.g., 128 bytes) and are not capable of sophisticated interactions.

2.2 WISP

Several RF energy harvesting techniques and prototypes were explored over the last few years. The WISP platform and its variants harvest energy from RFID reader [83] and TV radio stations [9], and are capable of powering an ultra-low-power microcontroller. The WISP was also used as a battery-less sensor node to communicate with a traditional RFID reader [83]. It relies on a high energy source (30 dBm) operating at a medium RF frequency (915 MHz). The constraint of the iPoint to operate on the low RF energy from smartphones (few dBm) and higher Wi-Fi frequency (i.e., 2.4 GHz) requires more advanced RF energy harvesting mechanisms that we present in the next sections. Other platforms for wireless power transfer exist but require either high transmission power on the 915 MHz band [69], or require highly customized

transmitters and receivers such as in wireless power transfer via strongly coupled magnetic resonances [50].

2.3 Backscattering

Communication based on RF backscattering has been an active avenue of research with application in medical sciences. In this form of communication, the transmitter sends RF signals to a passive device, normally implanted in the body. A receiver will measure the backscattered signal coming from the implant. With a careful design, one can modulate the information on the device in the backscattered signal. Researchers have shown a proof-of-concept design that can convert wireless transmissions from one technology (Bluetooth) to another (Wi-Fi, Zig-Bee) using backscatter communication via an implanted device [34]. Such design enables multimodal communication between implanted devices such as contact lenses and wearable devices equipped with multiple RF technologies in order to report medical or diagnostic information from the body.

2.4 Multi-path Energy Routing

Recent research [61] has shown promising results in transferring RF energy via a network of energy-harvester nodes. Energy can be routed alongside data in such networks. Within a network consisting of energy harvesters that are optimized to accumulate and relay the RF energy in different frequency bands, the energy flows along multiple paths increasing the overall harvesting efficiency.

2.5 Near-Field Communication (NFC)

The near-field communication (NFC) [62], founded by Nokia, Phillips, and Sony in 2004, is a set of standards based on RFID technology that allows devices such as smartphones to establish a communication. Communications take place at 13.56 MHz over very short range of less than few centimeters, which typically involves two devices touching each other. NFC allows several modes of communications including communication with a passive device. The communication scheme is ASK with Miller or Manchester coding. Data rate varies between 106 and 424 kbit/s. Because of the very simple and fast set-up, NFC can be used to initialize more sophisticated wireless communication to start peer-to-peer networking. The energy transfer mechanism is based on electrodynamic induction between two loop antennas. In comparison to the solution presented in this work, NFC exchanges data at higher data rates but operates at shorter ranges. Devices communicating over NFC normally needs to touch to

ensure reliability. Moreover, NFC functionality on a smartphone requires additional designated hardware, which adds another hardware dependency.

2.6 Bokode

Recently, a clever alternative solution to RFID tags and traditional barcodes, called bokode, was developed to deliver information from a dot of 3 mm diameter encapsulating a high-density Data Matrix code [60]. The information is revealed by putting an off-the-shelf camera in an out of focus mode. This solution has the advantage to reduce the size of the tag and increase the information density but still keeping the tag passive. However, bokode still lacks a two-way communication capability and requires sophisticated digital cameras (ten megapixel with a large lens) with in/out focus capability. In the future, if smartphones become equipped with controllable focus cameras, the envisioned iPoint system might benefit from integrating a bokode-based LCD display to deliver information to a smartphone at a lower energy cost.

2.7 Microwave Power Transmission

A mechanism based on RF energy harvesting has been explored to transfer a huge amount of energy over very long distances [58, 93]. For example, high-power directional antennas have been used to transmit energy to satellites from earth. The rectennas with efficiencies up to 95% have been demonstrated [85].

2.8 Resonant Inductive Coupling

Nonresonant inductive coupling, which is being widely used in transformers, suffers from stiff drop in efficiency when the distance between interacting coils increases. Karalis et al. [50] have shown that extremely high efficiency over mid-range can be achieved if the inductive coils couple in their resonant frequency. They have built a system that can transfer 60 W of power over distances up to 2 meters with 90% efficiency. Their work is the basis for a commercial technology called WiTricity [4] that promises efficient wireless power transfer that can be used to wirelessly power electronic devices within environments such as home or office. Several methods based on resonant inductive coupling have been proposed for wireless energy transfer in the biological setting, for instance to power medical implants in body [68, 73].

3 Consolidated Energy and Information Channels (CEICh) in Wireless Sensor Networks

In the previous section, we argued that combining energy and information transfer may provide an optimal solution to energy conservation in wireless sensor networks. In this section, we overview techniques to combine energy and information transfer channels in wireless sensor networks.

3.1 Overview of CEICh

First, we define the framework (model) in which CEICh is being implemented as follows:

- We consider a wireless sensor network whose nodes (devices) perform computations electronically and communicate using radio frequency (RF) signals.
- The network includes two types of nodes: passively powered receivers and the energy-provider master node, which we call the source.
- The communication only occurs between a source and a receiver at the time. We do not consider the communication among receiver nodes.
- In order to eliminate the energy conservation problem, the receiver may not rely on a battery or other unpredictable source of energy, such as solar energy or mechanical vibrations.
- In one communication cycle, the source sends the request to the receiver; the receiver receives the request, processes it, computes the reply, and sends it back to the source.
- The signal from source to receiver contains both energy and information. The receiver obtains the energy required to receive and decode the transmitted signal from the signal itself. Signals transmitted by receiver are not required to contain energy.

Figure 1 illustrates a general schematic of a CEICh.

3.2 Design of CEICh

A CEICh-enabled system performs three tasks: energy transfer, communication, and computation. In this section, we take a closer look into the important features and design elements of a CEICh enabled system.

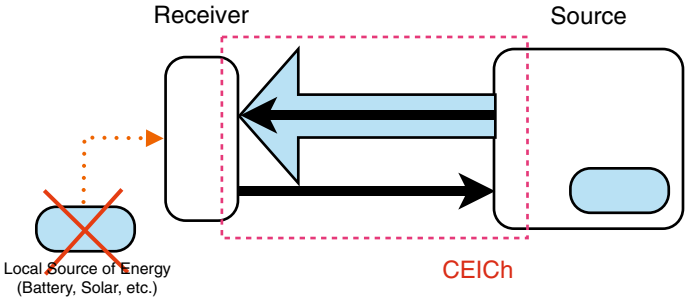

Fig. 1 The general schematic of CEICh

3.2.1 Energy Transfer Mechanisms

Mechanisms to transfer energy from a power source to a wireless device fall into two categories:

Electrodynamic Induction Methods based on electrodynamic induction use inductive coupling between the source and the receiver, and provide high-efficiency energy transfer over very short distances. In such systems, the efficient energy transfer occurs in the near-field region of the source's inductive antenna. The near-field region boundaries are determined by the size of the antenna and the wavelength of the transmission. For smaller antennas, the distances less than a wavelength, $R < \lambda$, from the source is considered near-field region, while the transition to far-field occurs in $\lambda < R < 2\lambda$. For larger antennas, the near-field region boundary is expressed by Fraunhofer distance:

$$R < \frac{2D^2}{\lambda}, \tag{1}$$

where D is the largest dimension of the antenna. The relationship between transmit power and the distance in the near field can be expressed as follows.

$$P_{\mathrm{T}} \propto \begin{cases} R^{-1} \text{ for } & R \leq 0.1\lambda \\ R^{-3} \text{ for } & R > 0.1\lambda \end{cases} \tag{2}$$

The efficiency declines significantly over greater distances, which makes such methods ineffective when the signal has high frequency and long range, a typical case in communications. Recently developed methods apply resonant inductive coupling to achieve much higher efficiency over longer ranges.

Electromagnetic Radiation Methods based on electromagnetic radiation, also called RF energy harvesting, include receivers equipped with *rectenna*, a specialized component made of an antenna connected to a voltage rectifier that converts the electromagnetic energy of the received signal to a usable DC voltage. These methods operate in far-field region of the corresponding antennas hence attain longer ranges. However, they exhibit a number of limitations. At the antenna level, a system

using omnidirectional antennas shows a quadratic drop in efficiency with respect to the distance. Moreover, the losses due to imperfect rectification and antenna matching reduces the efficiency of the system. Matching and rectification losses can be minimized in a well-designed rectenna. Also, the antenna efficiency improves using directional antennas and applying beam-forming techniques.

3.2.2 Energy Transfer Efficiency

The most important property of any energy transfer mechanism is the efficiency, that is what portion of the received energy from the source is converted to usable energy for the receiver side. The factors determining the overall efficiency of an energy transfer system is different depending on the method of transfer.

In case of electrodynamic induction, the overall efficiency is chiefly determined by mutual inductance between the interacting coils, which in general is given by the Neumann formula:

$$M_{ij} = \frac{\mu_0}{4\pi} \oint_{C_j} \oint_{C_i} \frac{\mathrm{d}s_i \cdot \mathrm{d}s_j}{|R_{ij}|} \tag{3}$$

where M_{ij} is the mutual inductance between coil i and coil j, μ_0 is the vacuum permeability, C_i and C_j denote the curve of the coils and R_{ij} is the distance between two points. The final value of the mutual inductance depends on the size of the resonators, their relative orientation, and the distance between them. The coupling coefficient between inductive resonators is defined as:

$$k = \frac{M_{ij}}{\sqrt{L_i L_j}}, \tag{4}$$

where L_i and L_j are self-inductance of the resonators. In many common inductive coupling systems, $0 < k < 1$ and the system is called weakly coupled. Using recent methods such as *Resonant Inductive Coupling*, one can achieve higher coupling factors ($k > 1$) and build strongly coupled inductive resonators. Other contributing factors in overall efficiency includes ohmic and core losses in the coils, and appropriate impedance matching at either side.

In energy harvesting systems, the overall energy transfer efficiency can be estimated by aggregating the effect of signal's transmission losses, impedance mismatch, and rectifier's energy efficiency. Signal transmission losses are given by Friis equation, which gives P_{R}, the power received at receiver's antenna:

$$P_{\mathrm{R}} = P_{\mathrm{T}} G_{\mathrm{t}} G_{\mathrm{r}} L_{\mathrm{p}} \left(\frac{\lambda}{4\pi R} \right)^2, \tag{5}$$

where P_{T} is transmit power; G_{t} and G_{r} are antenna gains at transmitter and receiver side, respectively; L_{p} is the polarization loss; λ is the wavelength, and R is the

distance between the antennas. Adding the effect of impedance mismatch, we can calculate the power that enters the rectifier circuit, P_{rec} as:

$$P_{\text{rec}} = (1 - |\Gamma_r|^2) P_{\text{R}}, \tag{6}$$

where Γ_{r} is the reflection coefficient of the receiving antenna. Finally, the input power to the receiver is given by:

$$P_{\text{in}} = \eta_{rec} \times P_{rec}, \tag{7}$$

where η_{rec} is the efficiency of the rectifying circuit. The value of η_{rec} depends on the design of the rectifier (e.g., half-wave or full-wave) as well as the electrical characteristics of its components such as forward and break voltages of the diodes and leakage voltage of the charging capacitors. In practice, the efficiency of the rectifier is measured experimentally since the exact calculation proves impractical due to complexity and nonlinearity of the circuit. In summary, the overall efficiency can be expressed as the following:

$$\eta = \frac{P_{\text{in}}}{P_{\text{T}}} = \eta_{\text{rec}} G_{\text{t}} G_{\text{r}} L_{\text{p}} \left(\frac{\lambda}{4\pi R} \right)^2 (1 - |\Gamma_{\text{r}}|^2). \tag{8}$$

Each of the contributing elements mentioned in Eq. 8 may be optimized to achieve higher energy transfer efficiency in the design of a CEICh. It is worth mentioning that Eq. 8 holds true assuming the perfect channel conditions. In practice, the efficiency is further affected by fading (F^{-1}), shadowing (B^{-1}), and on-object antenna gain penalties (Θ^{-1}), each of which can be either modeled or measured.

3.2.3 Signal Amplification

Another important factor in the design of a CEICh is the minimum voltage required to power-up the receiver, V_{min}. If the output voltage of the energy transfer unit is not sufficient, a voltage multiplier circuit may be used to elevate the voltage beyond V_{min}. Because of the limited energy budget, the voltage multiplication is done using a passive circuit. In energy harvesting mechanisms, signal rectification and amplification is done using voltage multipliers.

3.2.4 Voltage Rectification

A voltage rectifier, which is typically a network of diodes and capacitors, rectifies an input AC signal to output DC voltage. The simplest rectifying circuit is the envelope detector circuit shown in Fig. 2. Using a diode with forward voltage of V_{D}, the DC voltage of $V_{\text{out}} = |V_{\text{in}}| - V_{\text{D}}$ can be obtained in no-load conditions. The circuit

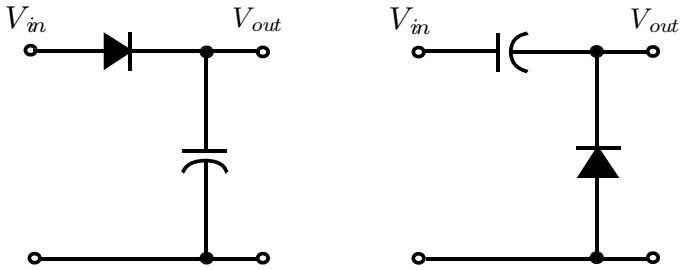

Fig. 2 The schematics of envelope detector circuit (left) and the clamp circuit (right)

experiences voltage ripples if connected to a load. This circuit is also called half-wave rectifier because only the positive half of the AC waveform is rectified.

A clamp circuit as shown in Fig. 2 may be used to achieve higher DC voltage levels. The negative half of the waveform is clamped to zero, and the output voltage of $V_{\text{out}} = 2|V_{\text{in}}| - V_{\text{D}}$ is obtained. The circuit, however, shows a very drastic ripple of size $2V_{\text{in}}$ when connected to a load.

By placing a clamp circuit in series with an envelope detector, one can achieve higher DC voltage levels and significantly improves the ripple characteristics of the circuit. This circuit, shown in Fig. 3, is called voltage doubler and was first invented by Heinrich Greinacher in 1913, and is later used to power the particle accelerators [16]. Let us look at the steady-state analysis of the voltage doubler circuit. On the negative half of the input AC waveform, the capacitor C_1 is charged until $V_{\text{C1}} = |V_{\text{in}}| - V_{\text{D}}$. Similarly, over the positive half, the capacitor C_2 is charged until we have

$$V_{\text{out}} = V_{\text{C2}} = |V_{\text{in}}| - V_{\text{D}} + V_{\text{C2}} \tag{9}$$

$$= 2(|V_{\text{in}}| - V_{\text{D}}) \tag{10}$$

The key feature of the Greinacher circuit is that individual voltage doublers can be cascaded to build a voltage multiplier that generates arbitrarily large output DC voltage. For an N-stage voltage multiplier, the output voltage of $V_{\text{out}} = 2N(|V_{\text{in}}| - V_{\text{D}})$ may be obtained theoretically. A output voltage can also be doubled by placing

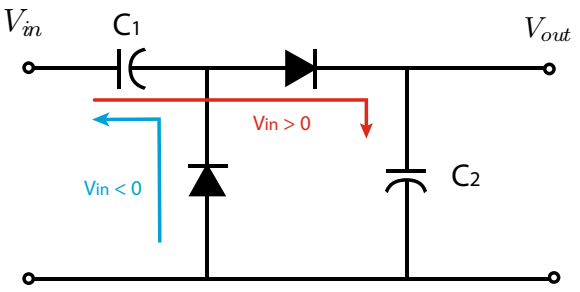

Fig. 3 Schematic of Greinacher voltage doubler

the voltage doubler in parallel with a mirrored copy with the same topology but reversed polarity of the diodes. In a careful design, the amount of ripple can be minimized when connecting the multiplier to a load. Note that, the analysis above assumes that the diodes and capacitors in the circuit are ideal in no-load conditions. In nonideal scenario, the parasitic effect of the capacitors in each stage and nonlinearity of the diodes significantly affects the performance of the voltage multiplier. Also, the behavior of the components will depend on the output current (load). There is no closed form for the efficiency of the system in realistic conditions. Therefore, the optimization of the overall efficiency of the rectifier should be based on simulation and experimental measurement.

3.2.5 Signal Characteristics

Incorporating energy transfer in communications requires modification in signal characteristics. Unlike conventional communication systems, the receiver does not include an active signal amplifier, therefore the transmitter has to provide a signal with higher level of energy to maintain the receiver in operating zone. In contrast, response signals do not have the aforementioned restriction since the master node does not have any energy constraints and may possess an active radio receiver with signal amplifier to receive and demodulate the response from the receiver.

Signal Preambles, Trailers, and Energy Storage In most cases, the converted power obtained from the signal is not sufficient for continuous operation of the receiver, hence the converted energy should be stored and accumulated over a longer period. In particular, the receiver needs to obtain a minimum amount of energy before it can demodulate the information. Therefore, the signal should include a *preamble* designed to provide the energy to start-up the receiver. Similarly, having received the signal, the receiver continues to process and respond to the request. The receiver should have already harvested enough energy to complete the tasks, otherwise, the signal needs to include a *trailer* that provides the required energy and may contain no actual information. We can define a duty cycle for the system which can be estimated by the following ratio:

$$DC = \frac{P_{\mathrm{ET}}}{P_{\mathrm{active}}} = \frac{\eta P_{\mathrm{T}}}{P_{\mathrm{active}}}, \tag{11}$$

where η is the energy transfer efficiency, P_{T} denotes the power sent by the transmitter, P_{ET} is the converted power from energy transfer unit, and P_{active} is the average power that the receiver requires to perform a communication cycle, that is, to start-up, demodulate, process, and reply to the signal. This unavoidable overhead significantly reduces the data rate and throughput of the communications in a CEICh.

3.2.6 Communications Schemes

Because of severe energy constraints, the demodulation process has to be simple as possible, while remaining effective. Sophisticated decoding mechanisms demand a significant amount of computations and energy, hence are not optimal. Due to integration of the energy transfer and communication, the signal from the master node to the receiver carries a considerable amount of energy. Therefore, the signal-to-noise ratio (SNR) is quite high, which allows using simpler modulation and demodulation schemes.

Most of today's communication protocols do not fulfill the requirements mentioned above, thus it needs to be modified or completely revamped according to the design requirement and constraints. For example, frequency-shift keying (FSK) and phase-shift keying (PSK) mechanisms require fairly complex receiver design, hence are not suitable for communication in CEICh. On the other hand, schemes such as amplitude-shift keying (ASK) or on-off keying (OOK) can be detected by a simpler receiver design (an envelope detector circuit), and consequently can be used in CEICh with minor modifications. Backscattering techniques are used to send information from the receiver to the source. Such techniques based on modulating information in the amplitude of reflected waves adjusting the impedance of the receiver's antenna, allow highly efficient bidirectional communication without using a stand-alone RF transmitter in the receiver. In the following section, we present a system that employs a two-way consolidated energy and information channel. The system includes two optimized communication protocols to achieve maximum energy efficiency.

4 IPoint

In this section, as an implementation of a CEICh-enabled wireless system, we propose a system that provides two-way communication between a receiver with no source of energy and a conventional smartphone. We present a complete design of the system featuring energy harvesting as the energy transfer method. We explore various technologies, introduce new communication paradigms, and build a prototype of the passively powered device that we call *iPoint*.

4.1 Motivation and Possible Applications

Providing information anytime, anywhere, and to anybody is a challenging task. Consider an application where we want to deliver information to any person equipped with a standard smartphone in even remote locations where there is no network coverage, and where no source of energy is available. The information should be

delivered from a device that can last decades without maintenance. Examples of applications include information delivery to hikers lost in the woods (e.g., directions, closest points for assistance), caves, and also high-density and interactive information tags (e.g., tourists information, museums).

A smartphone is an ultimate example of a wireless device. It provides a remarkable combination of data acquisition, computing power, and communication interfaces, all in a highly portable package. Our design exploits such capabilities of the smartphone to mitigate energy conservation issues.

4.2 Definition of the System with Respect to CEICh Design

iPoint is a passively powered device that is capable of communicating with a commodity smartphone while obtaining the required energy for computation and communication from the signal. This completely fits the definition of the receiver in our CEICh model. Here, the master node or the source is a smartphone. In the process of designing the iPoint, in addition to considerations stated in Sect. 3, we focused on the following key characteristics:

- *Universality*: any smartphone should be able to serve as the master node without any hardware modifications. Installing a software application should be sufficient to enable all desired functionalities.
- *Interactivity*: the device should be able to accept, process, and reply to specific requests. In other words, the communication between the iPoint and the smartphone is bidirectional.

4.3 Challenges and Approach

The key challenge to implement an efficient CEICh channel is sever power deficiency throughout the system. Smartphones, unlike RFID readers, are not capable of transmitting high-power RF signals. In fact, the amount of power transmitted by cell phones is aggressively controlled because of several FCC regulations health issues. Another obstacle that emerges in the course of the design, is lack of specialized wireless interfaces in the smartphone. To maintain the universality of the system, the CEICh design should use one of the standard wireless interfaces of the smartphone (GSM, Wi-Fi, and Bluetooth) without any hardware modifications. This eliminates the use of several mechanisms described in Sect. 3. For example, inductive coupling energy transfer may not be implemented since the majority of smartphones do not include inductive coupling resonator antenna.

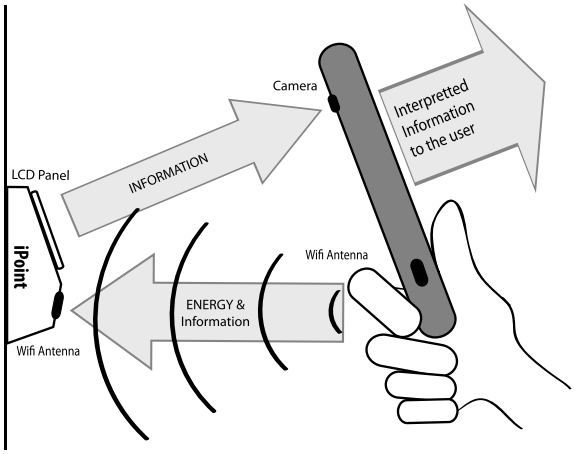

Fig. 4 Conceptual illustration of how iPoint device performs

4.4 Our Solution

These defining features lead us to a design that introduces innovative communication paradigms and techniques and the integration of a set of fairly unrelated technologies. Among the wireless interfaces present in smartphone, we picked Wi-Fi interface because it provides a greater degree of control by software, works on an unlicensed frequency band (2.4 GHz) and also has the highest transmit power. A backscattering technique cannot be used because of limited power budget and lack of compatible wireless interface to detect the backscattered signal in the smartphone. Instead, we design the iPoint to display the result on an LCD panel, exploiting the camera on the smartphone to acquire the data via the captured image of the display and interpret the information. Figure 4 shows how this design operates. In the following, we briefly review the system hardware and software architecture, the components, and the communication paradigms and techniques:

- *iPoint components*: the iPoint consists of a rectenna optimized for the 2.4 GHz Wi-Fi band, an ultra-low-power microcontroller with an LCD driver, and a multi-segment LCD panel.
- *Smartphone*: virtually any smartphone with a Wi-Fi network interface and an integrated camera.
- *Energy-provisioning*: the smartphone delivers the energy to the iPoint via Wi-Fi transmission. The iPoint benefits from a more efficient RF energy harvesting circuit optimized for limited transmission power of smartphones, about two orders of magnitude less than conventional RFID readers.
- *Multimodal communication*: we propose two novel communication mechanisms to circumvent the severe energy asymmetry and constraints. (1) The information from the smartphone to the iPoint is encoded in the Wi-Fi packet width, which results in much simpler and more energy-efficient demodulation at the expense of

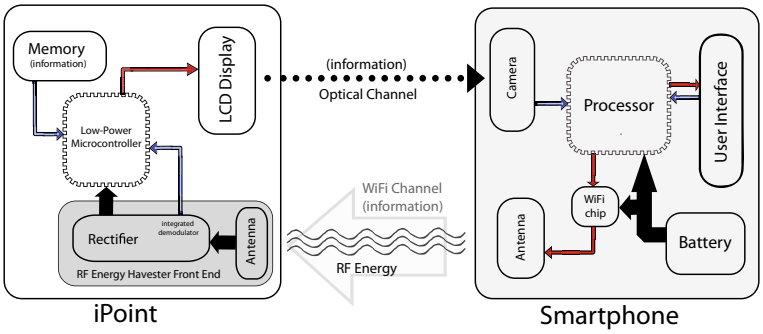

Fig. 5 Detailed diagram of iPoint

a lower data rate. (2) The information from the iPoint to the smartphone is encoded as a series of patterns shown on the LCD, to be captured by the smartphone camera.

4.5 Detailed System Architecture

This section outlines the architecture of the proposed system. We describe the system components in detail, discuss the required features, important parameters and trade-offs, and compare design choices. We break down hardware of the iPoint into three components: a rectenna that receives the information and energy, an ultra-low-power computing core to process the data, and a display to show the outputs (Fig. 5).

4.5.1 Energy Transfer

The energy transfer mechanism in iPhone is based on electromagnetic energy harvesting, therefore consists of a carefully design rectenna. The rectenna serves as the power supply for the device. Its two main components, the antenna and the rectifier circuit, in addition to two auxiliary circuits are described below:

- *Antenna*: The antenna is designed for the 2.4 GHz band. External whip antennas provide larger gain and better performance, whereas the integrated printed antenna make more compact design possible. The directionality of the antenna may be adjusted to achieve larger gain given spatial coordinates of the antenna with respect to the smartphone.
- *Rectifier circuit*: It converts the RF energy of the arrived Wi-Fi signals to DC voltage by passing them through a cascade of voltage multiplier circuits. Input power of the rectifier is often extremely small, therefore a multi-stage rectifier is used to build up sufficient output DC voltage, normally 1–5 V, to power the computing unit. The efficiency of the rectifier depends on the overall design of the circuit as

well as electrical characteristics of its components, notably forward voltage of the diodes and leakage of the capacitors. A full-wave rectifier shows better converting efficiency and produces more stable DC output compared to a half-wave rectifier, but requires a differential output design. Designs using Schottky diodes, which have smaller forward voltage, and RF optimized capacitors show significantly better performance.

- *Matching circuit*: The antenna and the rectifier should be carefully matched over the Wi-Fi frequency band. Matching is typically done by experiment. The trade-off between a good match and bandwidth of the rectenna should be considered in the design. The ideal bandwidth of the system is roughly 20 MHz, equal to width of the Wi-Fi channel.
- *Regulatory Circuit*: A shunt voltage regulator is placed after the rectifier is used to maintain the output DC voltage level within the safe range of operation for the computing unit.

Additionally, the rectenna constructs the envelope waveform of the arriving Wi-Fi transmission and passes it, as partially demodulated data, to the computing unit for further processing. We will discuss this in greater detail in Sect. 4.6.

4.5.2 Computation

The computing unit of the iPoint should provide extremely low-power consumption along with moderate computing capacity in a simple hardware design. Therefore, ultra-low-power microcontrollers (MCU), such as TI MSP430 family, are favorable design choices. The MCU should provide an adequate I/O interface and preferably include integrated drivers for external displays. Considering the energy constraints, the MCU may be underclocked to further reduce the power consumption.

4.5.3 Display

The iPoint displays the information with sufficient contrast and clarity to guarantee error-free pattern recognition by the smartphone, and minimize the energy consumption of the process. Passive-matrix liquid crystal displays (LCDs) [84] require a very small amount of energy to reach desirable contrasts without the need for a light source on the device, therefore is a better choice compared to LEDs. Given the same input voltage and distance from the camera, larger panels produce more pixels but less contrast compared to smaller panels.

4.6 Multimodal Communications

Because of the very low-power transmission of smartphones, the energy harvested by the rectenna is not sufficient to power a wireless transceiver and use conventional communication schemes. In this section, we describe two novel schemes that allow two-way communications between the iPoint and the smartphone within such limited energy levels. These schemes leverage smartphone capabilities to reduce the energy budget of the communications. We break down the communications into two separate channels: smartphone-to-iPoint (S2I) and iPoint-to-smartphone (I2S). We propose a different communication scheme for each channel.

4.6.1 Packet Length Modulation (PLM)

To provide energy for the iPoint device, the smartphone transmits Wi-Fi signals. However, demodulating Wi-Fi packets needs an active demodulator requiring energy beyond what iPoint harvester can obtain from the signals. We propose packet length modulation (PLM), a scheme in which the information is embedded in the length of the Wi-Fi packets.

Encoding In PLM, each packet length represents a symbol in the code. A message is defined as a sequence of Wi-Fi packets each representing its corresponding symbol. Note that, the smartphone sends the packets via its Wi-Fi interface, which uses the Wi-Fi protocol and does not know about the PLM. The following modifications to existing Wi-Fi protocol are necessary to implement PLM encoding functionality:

- Since a Wi-Fi access point may not be available, the smartphone creates an ad hoc Wi-Fi network.
- The iPoint lacks any Wi-Fi transceiver, hence no acknowledgment packet is sent back to the smartphone. Therefore, PLM uses broadcast packets to prevent unnecessary packet retransmission.
- The Wi-Fi packet length depends on the size of the packet, rate of the communication, and fragmentation. To have a robust encoding, the Wi-Fi interface should transmit at a fixed rate without using any rate-adaptation algorithm. This can be achieved by a UDP broadcast transmission.
- Assuming the PLM mechanism uses M different packet lengths, each packet encodes $\log_2 M$ bits of information. The fragmentation threshold determines the maximum packet length, hence the number of the symbols, and should be set to the maximum.

All modifications above are made in the software; no hardware modification is necessary.

Decoding To decode the PLM signal, the iPoint retrieves the length of the received Wi-Fi packets. First, the rectenna generates the envelope signal of the received Wi-Fi packet, and sends it to the computing unit. The computing unit samples the signal,

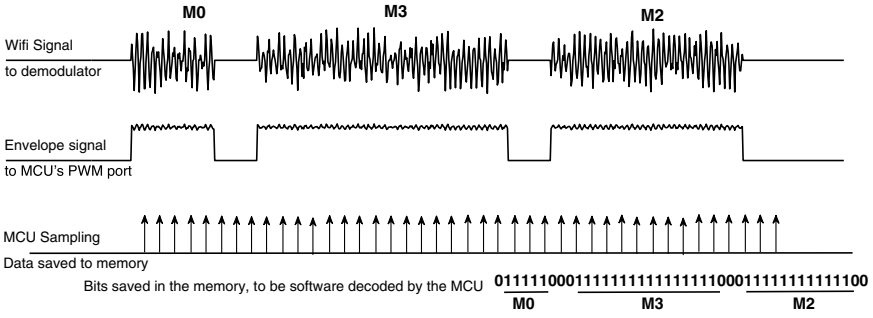

Fig. 6 PLM decoding

determines its length, and maps it to its corresponding symbol. Predefined start and stop flags can be used to distinguish the beginning and the end of a message. Figure 6 illustrates the steps of PLM decoding.

Data Rate Analysis Let M denote the number of the packet lengths in the PLM. Assume the transmitter sends the packets at rate, R. Let $S_{\min}$ be the smallest packet size. $S_{\min}$ is determined by the MCU clock to guarantee packet detection and length estimation, and by the energy-harvester efficiency and MCU energy requirements. We consider packets of size multiples of $S_{\min}$, $S_{\mathrm{i}} = i \times S_{\mathrm{m}in}$. Hence, the average size of the packet would be

$$S_{\mathrm{avg}} = \frac{S_{\min} + S_{\max}}{2} = \frac{(M+1)}{2} S_{\min}. \tag{12}$$

Further assume a message is a sequence of packets separated by *idle* periods of the length S_{idle}. We can calculate the time needed to send a packet, T_{p} and are as follows:

$$\begin{aligned} T_{\mathrm{p}} &= \frac{S_{\mathrm{avg}} + S_{\mathrm{idle}}}{R} \\ &= \frac{(M+1)S_{\min} + 2S_{\mathrm{idle}}}{2R} \end{aligned} \tag{13}$$

where R is the data rate of the Wi-Fi transmission in bps. Each packet encodes $\log_2 M$ bits of information. Therefore,

$$R_{\mathrm{PLM}} = \frac{\log_2 M}{T_{\mathrm{p}}} = \frac{2\log_2 M \times R}{(M+1)S_{\min} + 2S_{\mathrm{idle}}} \tag{14}$$

The values of $S_{\min}$ and S_{idle} are determined by the maximum sampling rate of the MCU at iPoint side. Assuming f_{MCU} is the sampling frequency of the MCU, we have

$$S_{\min}, S_{\mathrm{idle}} > \frac{2R}{f_{\mathrm{MCU}}} \qquad \text{(Nyquist theorem)}. \tag{15}$$

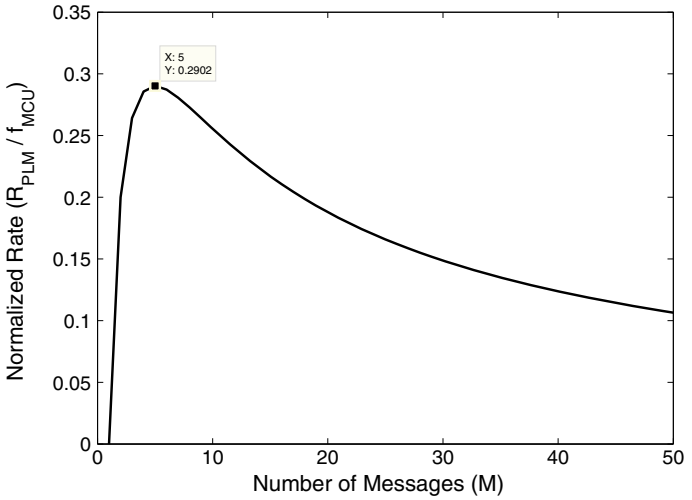

Fig. 7 Normalized Rate of PLM for different number of messages. It is shown that the best performance is achieved when $M = 5$

Hence,

$$R_{\text{PLM}} < \frac{2R \log_2 M}{(M+1)(\frac{2R}{f_{\text{MCU}}}) + 2(\frac{2R}{f_{\text{MCU}}})} \tag{16}$$

$$R_{\text{PLM}} < \frac{\log_2 M \times f_{\text{MCU}}}{M+3}. \tag{17}$$

Figure 7 illustrates the performance of the PLM for different values of M, showing that the best performance is achieved using five different packet lengths. Note that during idle periods, iPoint does not receive energy from the smartphone. This lowers the output voltage of the rectifier which may result in unwanted shutdown of the system. To maintain the harvested voltage level above the desired threshold, S_{min} needs to be larger than S_{idle}. We define the duty cycle of the PLM as the $S_{\text{min}}/S_{\text{idle}}$ ratio. The minimum duty cycle that allows the system to operate continuously depends on the implementation and may be evaluated experimentally. Moreover, $S_{\text{max}} = M \times S_{\text{min}}$ should be smaller than the fragmentation threshold in the smartphone Wi-Fi interface.

Finally, the smartphone needs to send preamble and trail Wi-Fi packets to provide the energy required for the iPoint to start-up, process the information and send the reply message back through I2S channel.

Bit Error Rate of PLM Before we start to estimate the bit error rate (BER) of the PLM, let us take a closer look at the decoding mechanism. As previously explained, messages are separated with an idle period of length $S_{\text{idle}} = S_{\text{min}}$. Let us assume that MCU records N samples during that period. The sample is considered low (OFF) if

the recorded voltage is below a threshold (V_{th}), otherwise is recorded as high (ON). PLM decoder uses a sliding window to detect the S_{idle} while counting the recorded samples. The decoder detects S_{idle} when more than $\lfloor N/2 + 1 \rfloor$ samples in the window are recorded as OFF. Once S_{idle} is detected, the number of the samples up to that point determines the preceding message. Given this decision mechanism, there are two possible scenarios that the decoder receives an incorrect message:

CASE I: If the decoder fails to detect an idle period. In this case, two messages around the undetected idle period are both lost.
CASE II: If the decoder mistakenly detects an idle period in the middle of a message. In this case, the incoming message is lost.

First, we estimate the probabilities of sample error. Because of the close proximity of the communication entities and presence of line of sight, we model the channel between source and the receiver as additive white Gaussian noise (AWGN) channel with good approximation. Therefore, the received sample, y can be expressed as $y = s + n$, where n is the noise estimated by a zero-mean normal distribution with variance of N_0. During the idle period, the input of the envelope detector is the white noise, n. If Gaussian noise is passed through an envelope detector, the probability density function (PDF) of the envelope of the noise at the output of the detector can be estimated with the following Rayleigh density function [70]:

$$P(x) = \frac{x}{N_0} e^{-x^2/2N_0} \tag{18}$$

Therefore, the probability of the error (Blue area as shown in Fig. 8) is given by:

$$P(e|s_{\text{off}}) = P(x > V_{\text{th}}) = \int_{V_{\text{th}}}^{\infty} \frac{x}{N_0} e^{-x^2/2N_0}\, dx. \tag{19}$$

When the signal is present, the PDF of the output of envelope detector can be estimated by Rician distribution [72]. Assuming that the amplitude of the signal is A, we have

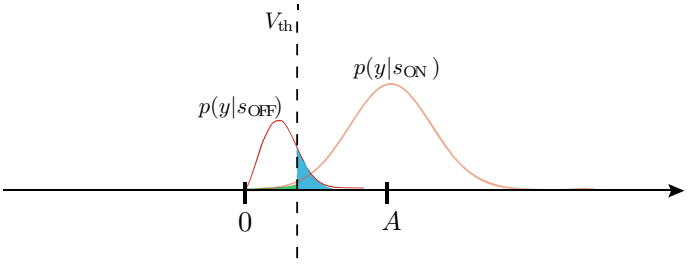

Fig. 8 Probability density function of the received sample with PLM modulation

$$P(x|A) = \frac{x}{N_0} e^{-(x^2+A^2)/2N_0} I_0\left(\frac{xA}{N_0}\right), \tag{20}$$

where I_0 is modified Bessel function of order zero. The sample error occurs when detected envelope falls below voltage threshold and has the following probability (Green area as shown in Fig. 8):

$$P(e|s_{\text{on}}) = P(x < V_{\text{th}}) = \int_0^{V_{\text{th}}} \frac{x}{N_0} e^{-(x^2+A^2)/2N_0} I_0\left(\frac{xA}{N_0}\right) dx \tag{21}$$

Also, samples are independent and identically distributed (i.i.d.). Consequently, the probability of *CASE I*, that is when more than $\lfloor N/2 + 1 \rfloor$ samples that were sent as s_{off} are detected as s_{on}, can be calculated as the following.

$$p_{\text{I}} = \sum_{i=\lfloor N/2+1 \rfloor}^{N} p(e|s_{\text{off}})^i (1 - p(e|s_{\text{off}}))^{N-i}, \tag{22}$$

where $p(e|s_{\text{off}})$ is the probability of an error given an OFF sample was transmitted. In *CASE II*, the probability of error in a message of length $m \times S_{\text{idle}}$ is:

$$p_{\text{II}}^{\text{m}} = (1 + (m-1)N) \sum_{i=\lfloor N/2+1 \rfloor}^{N} p(e|s_{\text{on}})^i (1 - p(e|s_{\text{off}}))^{N-i}. \tag{23}$$

The total probability of CASE II can be calculated by averaging over all the message sizes. For PLM with M different message, we have

$$p_{\text{II}} = (1 + \frac{(M-1)N}{2}) \sum_{i=\lfloor N/2+1 \rfloor}^{N} p(e|s_{\text{on}})^i (1 - p(e|s_{\text{off}}))^{N-i}. \tag{24}$$

We assume that the probability of sending ON and OFF messages are equal $p(ON) = p(OFF) = 0.5$. Each message codes $\log_2 M$. Therefore, the total BER can be written as:

$$BER = \frac{1}{2} \log_2 M (2p_{\text{I}} + p_{\text{II}}) \tag{25}$$

Interference The scale of the PLM performance degradation due to interference is limited because the device operates in short range. The sources of Wi-Fi interference with large output power (e.g., access points or RFID readers) are commonly located far from the device and as a result, do not pose any disruptive interference.

4.6.2 LCD Pattern Coding (LPC)

The transmitting power of the smartphone is much lower than a conventional RFID reader (few milliwatts for the smartphone versus few watts for the RFID reader). Therefore, using a similar scheme as passive RFID tags (i.e., backscattering) is not practical. Instead, we introduce LPC, a low-cost way of sending information to the smartphone taking advantage of the imaging and computing capability of the phone.

Encoding Having processed the request sent from the user, iPoint encodes the information in a series of LCD segment patterns and displays them on the panel. The smartphone captures the sequence of the patterns with the camera, recognizes the patterns, interprets the information, and finally sends the interpreted data to the user through its own UI. Because all the expensive operations are done on the smartphone side, the encoder/transmitter complexity of the iPoint may reduce significantly. This also proves to be a very energy-efficient method as displaying information on the LCD panel requires far less energy compared to conventional back scattering scheme used in passive RFID tags. To get an intuition about the energy efficiency of LCD displays, one can think of the lifespan of wrist watches with LCD display; they run for years on a tiny button cell holding a small amount of charge.

An LCD pattern is a combination of the LCD display's segments where a segment can be ON or OFF. Upon receiving a request, the MCU computes the LPC encoded output message, as a sequence of predefined patterns to be shown on the LCD panel. A two-dimensional (2D) barcode encoding such as QR codes may be used to encode the information. An LPC message that consists of n patterns on a M-segment LCD panel, encodes $n \times M$ bits of information (Fig. 9).

Decoding At the other end of the channel, the LPC message is captured by the smartphone camera by either recording a video or taking a series of pictures at a satisfying rate. The smartphone decodes the captured message by running a pattern recognition algorithm on each frame, and sends the interpreted data to the user via UI or uses the data in the next sessions of communication. Several 2D barcode decoding algorithm and software for smartphones have been published [24]. An example of such setting is shown in Fig. 10.

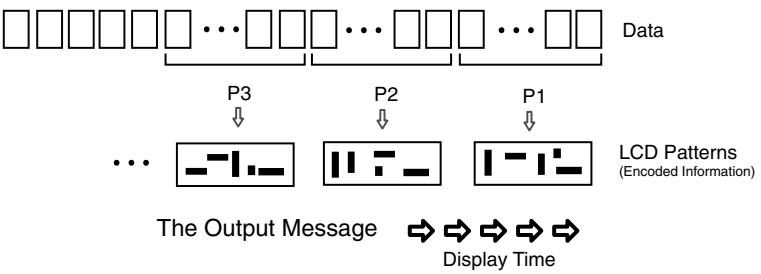

Fig. 9 LPC Encoding for a M-segment LCD panel

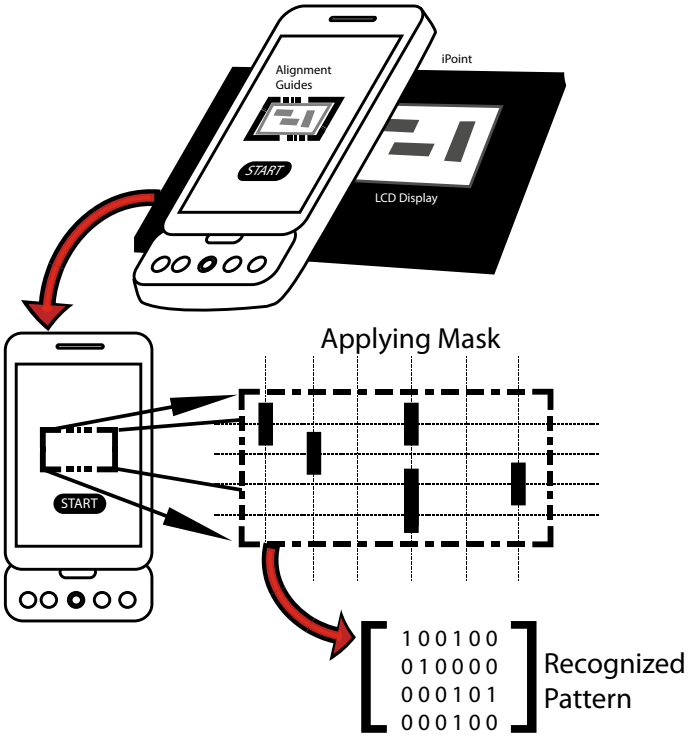

Fig. 10 LPC decoding. To make decoding faster, the user is asked to align the image of the panel within a virtual box, then the frame is sampled only on the intersections of mask grid lines (Narrow dashed lines)

LPC Rate Analysis: Using passive-matrix panels, the LCD pattern update rate can go up to 200 Hz. However, our experiments indicate that the deciding factor on an error-free decoding is the sampling rate of the camera. Let R_c denote the maximum sampling rate of the smartphone camera. Applying Nyquist theorem, we have, $R_{max} < R_c/2$ fps. Therefore, for a M-segment LCD display, we have the upper bound transmission rate of $R_c M/2$ bps. For most of today's commercial smartphone cameras, $R_c \approx 30$ fps.

4.7 Optimization Techniques

In this section, we take a closer look into the techniques to optimize the performance of the iPoint. We review the design choices for each component of the system, and present advantages and disadvantages for each design. Also, we study the trade-offs that emerge in the course of the hardware and software design.

4.7.1 Antenna

The antenna is a key component of the iPoint design and its performance has a major impact on the overall efficiency of the system. Note that in any communication system, the design of both receiver and transmitter antenna should be optimized. However, in order to maintain universality in our design, we do not have any control over the transmitting antenna on the smartphone. Therefore, we assume that the smartphone is equipped with an omnidirectional antenna optimized for the Wi-Fi frequency and focus on improving the receiving antenna. In the design of iPoint, we aim to maximize the gain of the antenna as well as its radiation performance over the operating frequency band, which is 2.4 GHz for iPoint. The cost and size of the antenna plays an important role in choosing the proper antenna design. There are three main types of antennas that can be used in our design: whip antennas, chip antennas, and PCB planar antennas. Whip antennas consist of a single straight piece of conductor, normally in the form of a wire, mounted over the ground plane. These antennas have the simplest design and can achieve high gains (up to ≈ 6 dBi). However, they should extend perpendicular to the ground plain and the board to achieve the best performance, hence, are not easily fit in compact board designs. Chip antennas are smaller and can be easily mounted on electronic boards, but have a radiation performance ranging from mediocre to poor. PCB antennas provide the most flexibility in terms of antenna geometry. They are planar and have small size in high frequencies therefore can fit in compact designs. The RF performance of the PCB antennas are typically worse than whip antennas, but a good performance can be achieved with a careful design using microwave simulation tools. In the following, we present three PCB antennas that we designed for iPoint. We list the characteristics, advantages, and disadvantages of each design.

PCB Dipole Antenna Dipole antennas have been widely used since the early days of radio. Simplicity and effectiveness for a wide range of communication needs are the reasons for this. A dipole, which it gets its name from its two halves, is a balanced antenna, meaning that the poles are symmetrical: they have equal lengths and are extended in opposite directions from the feed point. To be resonant, a dipole must be electrically a half wavelength long at the operating frequency. Figure 11 shows the geometry of our dipole antenna which is designed to operate at 2.4 GHz. The return loss S_{11} of this antenna is presented in Fig. 11.

Yagi–Uda Antennas Higher gain antennas are usually obtained by forming arrays of basic antennas. The Yagi–Uda antenna is the most successful general-purpose directional antenna design at frequencies up to 2.5 GHz. It is inexpensive and simple to construct, and will provide gains of up to about 17 dBi. Yagi–Uda antennas can be built to support high input powers, and they are commonly used for directional broadcast transmission. The geometry of the designed Yagi–Uda antenna, which is operating at 2.4 GHz, is shown in Fig. 12. The return loss of this antenna is also illustrated in Fig. 12. The gain and directionality of Yagi–Uda antennas are particularly desirable. However, their large size in our operating frequency becomes problematic and renders their use impractical.

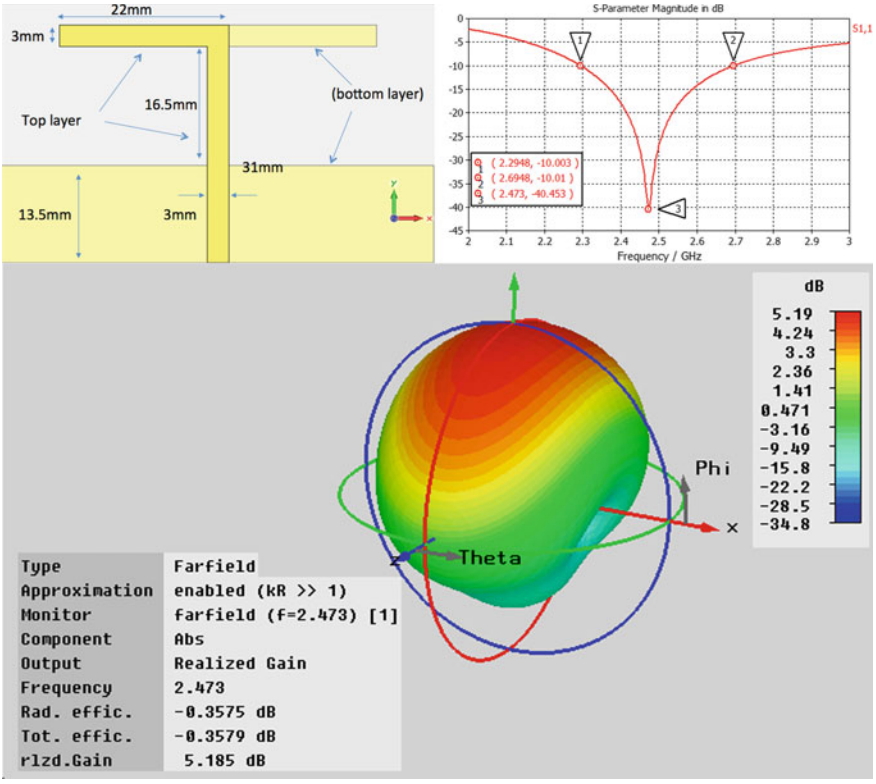

Fig. 11 The design of our dipole antenna optimized for 2.4 GHz [37]

Planar Inverted-F Antenna The planar inverted-F antennas (PIFA) are commonly used in mobile communication devices due to their small size (quarter-wavelength). These antennas typically consist of a rectangular planar element located above a ground plane, a short-circuiting plate, and a feeding mechanism for the planar element. The Inverted-F antenna is a variant of the monopole where the top section has been folded down so as to be parallel with the ground plane. This is done to reduce the height of the antenna, while maintaining a resonant trace length. This parallel section introduces capacitance to the input impedance of the antenna, which is compensated by implementing a short-circuit stub. The stub's end is connected to the ground plane through a via connection. Figure 13 shows the geometry of our PIFA antenna designed to operate at 2.4 GHz [37]. The return loss of this antenna is also shown in Fig. 13. PIFA's size makes it a very good choice for compact board design, however, its performance is subpar compared to dipole and Yagi–Uda antennas.

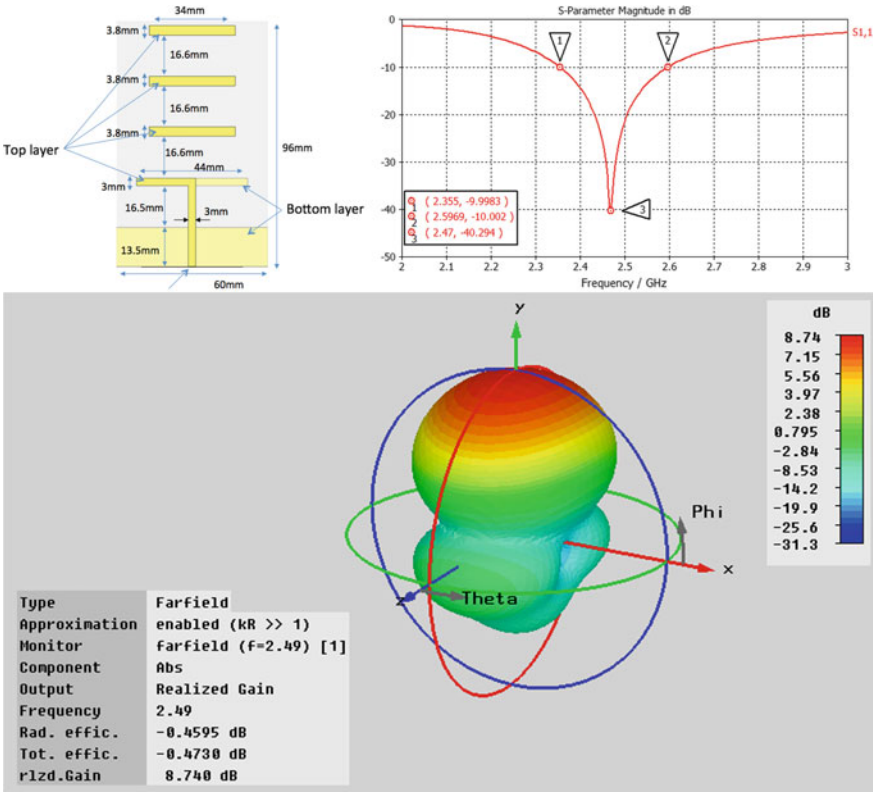

Fig. 12 The design of the Yagi–Uda antenna array optimized for 2.4 GHz

4.7.2 Rectifier

The rectifier designed for iPoint is based on multi-stage Greinacher circuit described in Sect. 3.2.4. The overall efficiency of the rectifier is determined by combination of the design of the rectifier and the electrical characteristics of its components. In this section, we review the key elements in designing an optimized rectifier for iPoint.

Diodes Since the rectifier is used to convert high-frequency Wi-Fi signals, the diode used in the design should have fast switching times. Among available types of diodes, Schottky diodes provide the fastest switching time, therefore are most suitable for RF energy harvesting. Another benefit of using Schottky diodes is their low forward voltage (150–350 mV), which is considerably lower than normal p–n junction diodes (0.6 V). The lower forward voltage allows a greater portion of the signal to be rectified and directly improves the efficiency of the rectifier. Other important parameters that need to be considered in picking the proper diode for the design is the saturation current, junction capacitance, and series resistance. In particular, we are looking for the following characteristics:

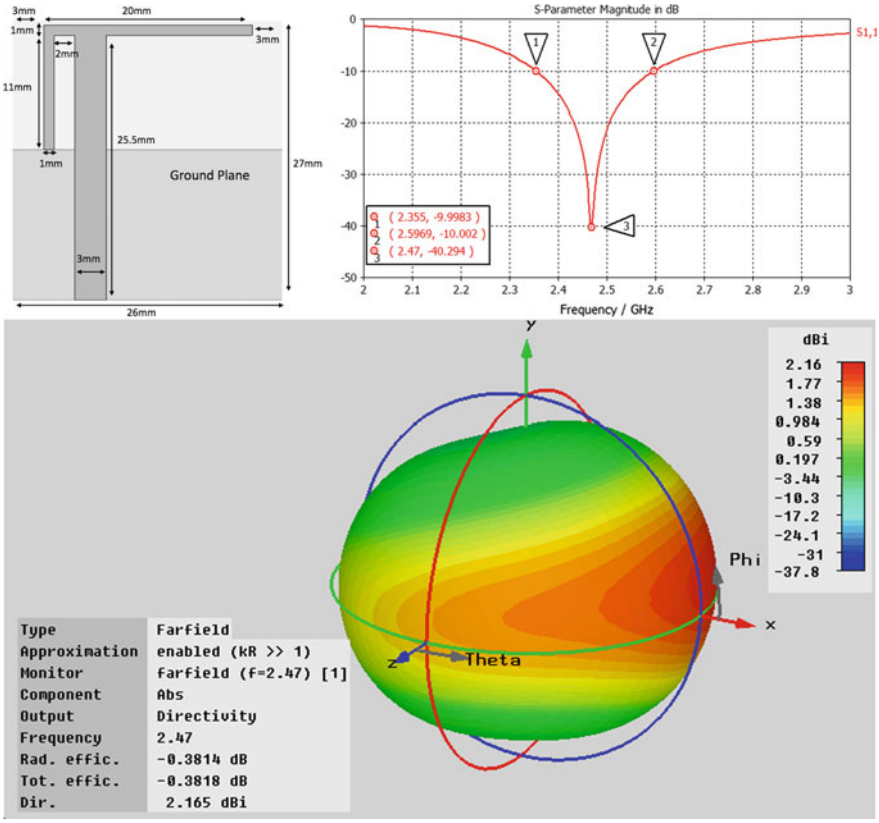

Fig. 13 The design of the Planar Inverted-F Antenna optimized for 2.4 GHz

- High saturation current is required for driving heavier loads.
- Lower junction capacitance leads to lower overall rectifier reactance and reduces the frequency dependence of the rectifier, and consequently eases the impedance matching.
- Lower series resistance is desirable in order to reduce the power loss within the rectifier.

In our prototype, we use HSMS-282x Schottky diodes from Avago Technologies since they provide the best combination of the electrical characteristics within the operating frequency and power band.

Load Impedance As described before, the load impedance greatly affects the performance of the rectifier. The impedance of the MCU computing core of the iPoint varies depending on the state of the computation. The low-power mode (LPM) of the MCU shows the highest impedance, whereas the lowest impedance was measured when MCU was driving the LCD. The highest power consumption coincides with

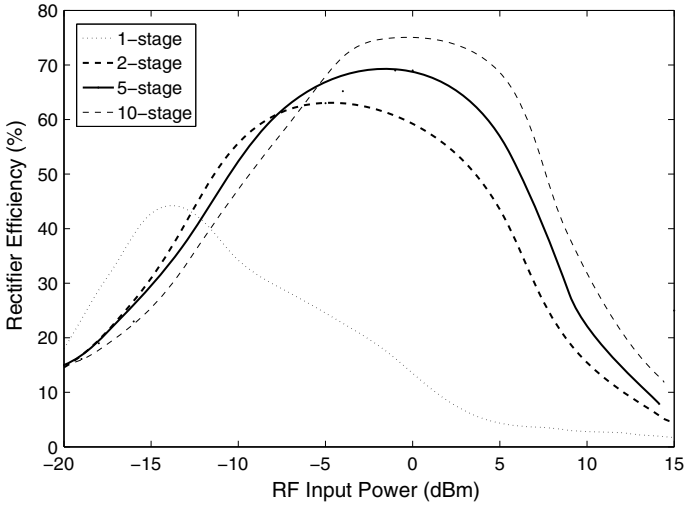

Fig. 14 Rectifier efficiency versus Input power for different number of the stages

the lowest impedance of the MCU, measured as 140 kΩ; In order to ensure that the rectifier provides necessary power at all times, we modify the rectifier to have the best efficiency while driving the maximum load.

Rectifier Topology The number of the stages and RF input of the rectifier have significant effect on the output voltage level and efficiency of the rectifier.
Number of Stages In an ideal multi-stage rectifier, the output voltage is proportional to number of the stages. Nevertheless, that does not hold in practice. The parasitic effects of the intermediate stages plus the power loss due to resistance in each stage limits the practical number of stages. Obtaining a closed-form analytical solution in a multi-stage rectifier is not practical, but the optimization can be done using realistic simulation. We used Agilent ADS tool to simulate rectifiers with different number of stages. The components of each circuit are identical and simulated using the vendor-provided parameters. Figure 14 shows the efficiency of the rectifiers versus input RF power. It shows that the maximum efficiency of the rectifier improves as number of stages grows. The simulation result also shows that rectifiers with higher number of stages show better efficiency at higher input powers.

4.7.3 Matching Strategy

The goal of the matching network is to adjust the input impedance of the system seen from the antenna-rectifier interface, Z_{in}, in order to have

$$Z_{\text{in}} = Z_{\text{ant}}^{*}. \tag{26}$$

Here, lies a peculiar problem: the diodes are nonlinear electrical components, hence the rectifier circuit shows a collective nonlinear behavior. This implies that Z_{in} depends on the input power from antenna, P_{R}. This is not an ideal situation because P_{R} may vary unpredictably due to numerous dependencies discussed in Sect. 3.2.2. The dynamic input impedance calls for a dynamic and adaptive matching mechanism that cannot be achieved using passive components.

A viable solution to minimize the effect of impedance mismatch is to measure the variation of Z_{in} for a reasonable range of input power and design the matching circuit accordingly. In the case of iPoint, we assume that the smartphone is always transmitting Wi-Fi signals at the maximum power allowed by regulations. Therefore, the optimal matching occurs when the communication occurs in a specific distance, which can be predicted.

The problem of dynamic impedance remains even if the input power is constant. This is because the input impedance of the system is also affected by the current that computing unit draws from the rectenna, i_{out}. For example, the MCU requires significantly higher current in the active mode (i.e., performing computation) compared to standby (i.e., low-power mode), which results in lower input impedance. If matching is optimized for the standby mode, any increase in i_{out} results in quick drop of output voltage of the rectifier leading to system shutdown. A partial solution is to match the rectenna for an desired input impedance, which in most cases is minimum value of Z_{in} when $i_{\text{out}} = max$. Given a fixed input power, when i_{out} falls below maximum value, a power mismatch occurs but in fact the output voltage of the rectifier increases. This prevents the system from shutting down as long as the input power is sufficient.

In our design, matching is done using an LC network plugged between the antenna and the rectifier. The final trade-off in matching is the operating bandwidth of the system. While high-quality sharp matching maximizes the power transfer efficiency, it also makes the system more frequency selective. This might not be ideal where the operating bandwidth of the system is not small. The fundamental limit of impedance matching over a bandwidth can be estimated by Bode-Fano theorem. Let us assume the rectifier circuit can be represented by a parallel RC network. According to Bode and Fano, if a lossless matching network is employed, we have the following limit on the reflection coefficient for different frequencies:

$$\int_0^\infty \ln\left(\frac{1}{|\Gamma|}\right) \mathrm{d}\omega \leq \frac{\pi}{RC}. \tag{27}$$

A perfect matching over a specific bandwidth $\Delta\omega = \omega_2 - \omega_1$ is theoretically achieved if $\Gamma = 1$ for frequencies outside the bandwidth and $\Gamma = \Gamma_{\text{min}}$ for $\omega_1 < \omega < \omega_2$. Equation 27 gives the following lower bound for operating reflection coefficient:

$$\Gamma_{\text{min}} > e^{-\pi/RC\Delta\omega}. \tag{28}$$

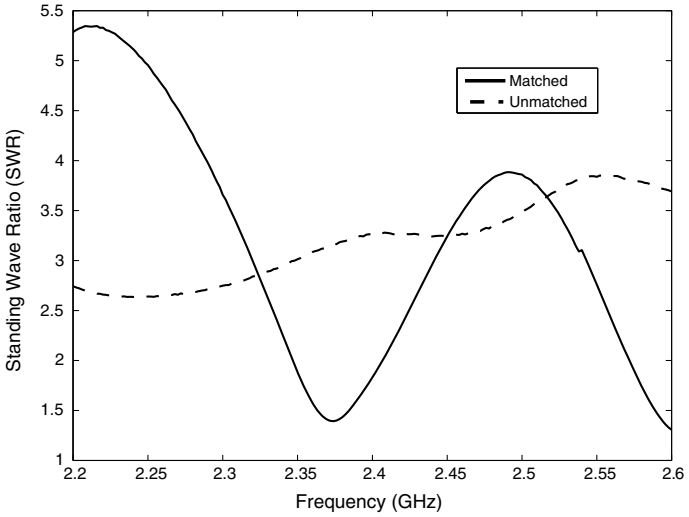

Fig. 15 The impedance matching in action. The standing-wave ratio (SWR) of the rectenna is shown before and after careful matching at active mode load

Dynamic impedance of the system makes the matching mechanism a very complex problem. As previously explained, the efficiency of the rectifier is also dynamic and shares some of the same dependencies. In practice, it is necessary to determine the value of matching components by optimizing the output power of the rectenna, which accounts for both matching and rectifying efficiency. Figure 15 shows the performance of the designed matching network for iPoint's rectenna.

4.7.4 Low-Power Computation

Power-aware Software The embedded software of the iPoint takes advantage of low-power modes (LPM) provided by MCU to minimize the power consumption. Any MCU components (timer, ADC, etc.,) can be turned off when its functionality is not required.

Underclocking To further reduce the power consumption of the computing core, we aggressively underclock the MCU. The iPoint's computing core tasks, such as PLM decoding and LPC encoding, do not demand a very fast clock, hence the clock frequency may be reduced to a few kilohertzs. Figure 16 illustrates the results of our measurements of the MCU's power consumption running the same instructions at different clock frequencies.

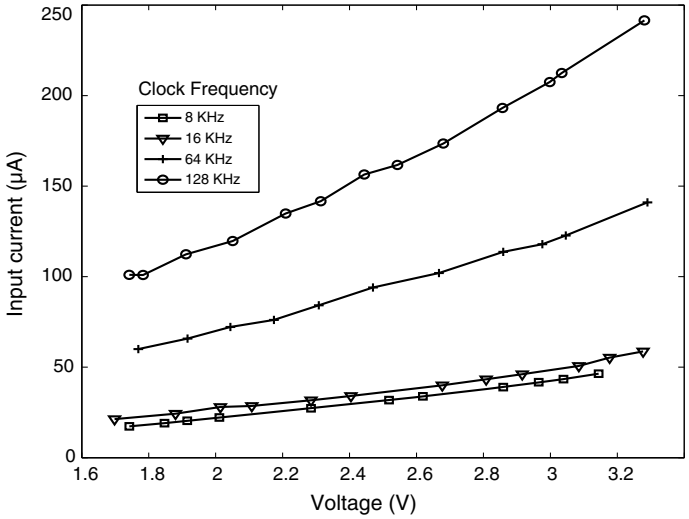

Fig. 16 Power consumption of MCU for different clock frequencies

4.7.5 Prototype

We prototyped different versions of the iPoint based on the design described in Sect. 4.5. Two versions (Ver. 2.1 and 3.1) are shown in Fig. 17. In this section, we explain the implementation of the components in detail.

The smartphone used in the experiments is the *HTC Dream* also known as *T-Mobile G1* running Android mobile device platform Ver. 1.6. This 3G phone is equipped with a 528 MHz Qualcomm ARM11 Processor, 192 MB of DDR SDRAM, 320×480 pixel LCD Display with 180 ppi, 3.2-megapixel camera with auto-focus capability, and a Wi-Fi (802.11 b/g) wireless interface [35]. We developed a software application in Android platform that sends multiple PLM-modulated requests, and performs the LPC decoding. The Wi-Fi interface was configured to send broadcast packets at a fixed rate of 1 Mbps, the lowest rate supported by Wi-Fi communication. Ideally, the application should create an ad hoc network, but the Android's support for the ad hoc mode is currently limited. As an alternative solution for prototyping, the smartphone connects to an auxiliary Wi-Fi network created by an external access point. We use UDP/IP, as opposed to TCP/IP, to avoid unnecessary retransmissions caused by TCP flow control mechanism. For the iPoint rectenna, we implemented a ten-stage modified Greinacher circuit, a full-wave rectifier with parallel RF inputs connected to a 2.4 GHz whip antenna. We used high-performance low-leakage RF capacitors, and Schottky diodes (HSMS-282 series from Avago technologies) with forward voltage threshold of 150–200 mV, the lowest available. The value of intermediate capacitors were chosen experimentally to maximize the output DC voltage. The rectenna then was matched on Wi-Fi channel 1 (2.412 GHz) using an LC matching network. The first stage of the rectifier circuit was used as an envelope detector

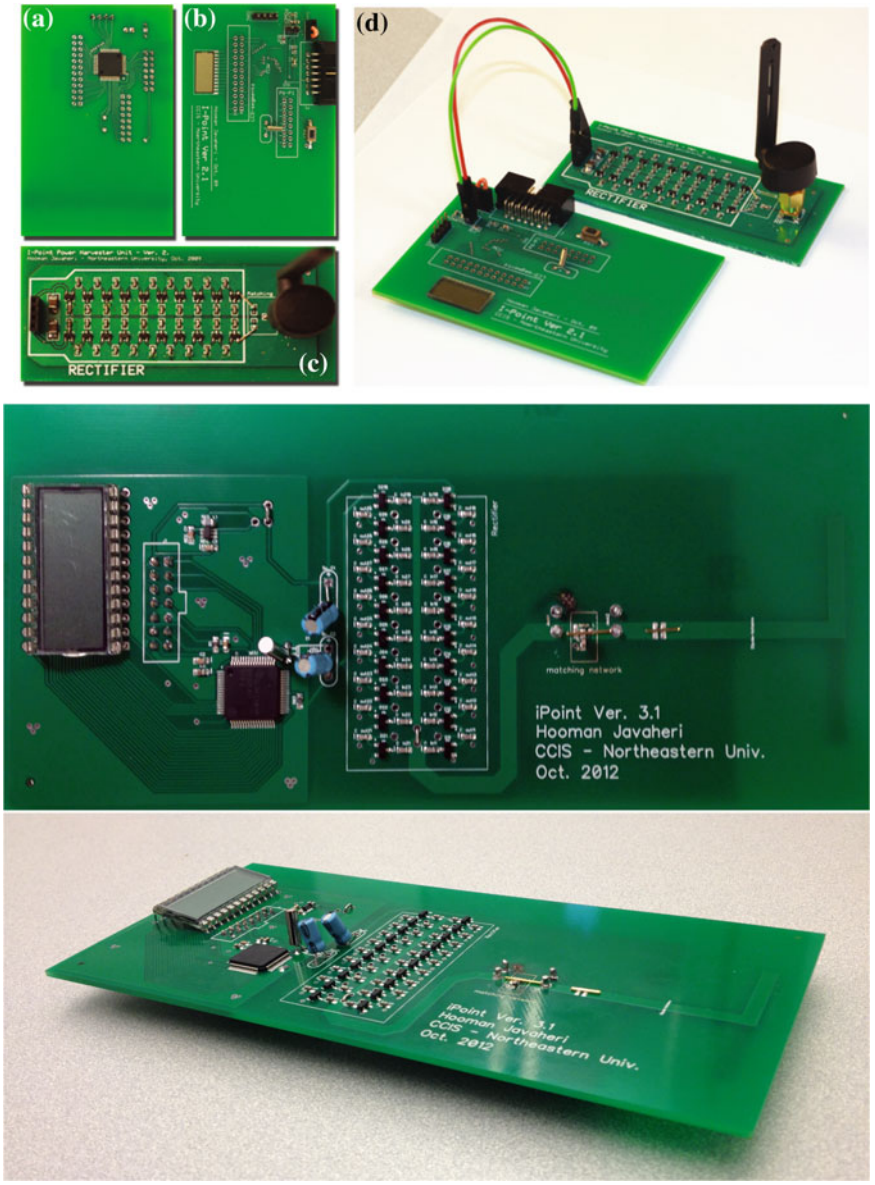

Fig. 17 The Prototype of iPoint. *Top*: The iPoint prototype boards: **a** Computing core upper layer (LCD display is shown). **b** Computing core lower layer (MSP430 is shown). **c** RF energy-harvester front end, ten-stage Greinacher voltage multiplier. **d** The realization of iPoint version 2.1. *Middle*: Prototype Version 3.1 with unified board design and PCB antenna. *Bottom*: Low-profile design of the iPoint Ver. 3.1

circuit for PLM decoding. For the communication core, we embed a TI MSP430F417, an ultra-low-power microcontroller from Texas Instruments. This 16-bit flash MCU provides desired computing capabilities at low-power consumption. It features 32 kB + 256 B of flash memory, 1 kB of RAM, Low supply voltage of 1.8 V, integrated LCD driver for 96 segments, on-chip comparator that can be used for finalizing the PLM signal demodulation, and very low active power consumption of 200 μA at 1 MHz, which makes it a reasonable choice for the iPoint prototype. The LCD panel selected for this generation of the prototype was a 26 segment watch LCD display.

4.7.6 Performance Evaluation

We carried out several experimental measurements in order to accurately characterize the device and prove the functionality of the design components. This section presents the detailed description of the testbed and experimental results.

Range Based on our experiment, iPoint requires around −10 dBm of power to operate normally. The transmit power of Wi-Fi interface of smartphones varies from a model to another but can be roughly estimated between 10–20 dBm. If the antennas at both receiver and transmitter side provide gain of $G_T = G_R \approx 3$ dB, and we have polarization mismatch of $L \approx -3$ dB, the link budget analysis gives an operating range up to two times of the signal wavelength, which is 12.5 cm for Wi-Fi signal. Our experimental evaluation is in agreement with the preceding estimation; our prototype was fully operational in ranges below 25 cm.

Rectifier Efficiency To characterize the efficiency of the rectifier circuit, a MXG Vector Signal Generator was used to feed the rectifier via a 0.5 ft coaxial cable, and the output voltage level of the rectenna was measured. The rectifier was fed with a Wi-Fi signal in a wide range of input power, from −20 dBm to 15 dBm. The output voltage and efficiency were measured without a load and with a load of 140 kΩ, which is close to the MCU impedance in active mode. Rectifier shows efficiency levels up to 72%. The results are shown in Figs. 18 and 19.

Duty Cycle of PLM Minimum duty cycle as one of the important characteristics of the iPoint system was discussed in Sect. 4.5. We measured the output DC voltage of the rectenna for different duty cycles. The results are summarized in Fig. 20.

LCD Contrast Test The accuracy of LPC decoding relies on the contrast of the pattern shown on the LCD panel, light conditions and the distance of the camera from the panel. If available on the smartphone, an LED flash may be used to compensate low-light conditions.

The power consumption of two LCD panels with different sizes were measured: Panel 1 (3 cm^2, 24 segment) and Panel 2 (1.8 cm^2, 26 Segments). A test image was taken from the LCD panels at the same distance and under the same light environment while the same pattern were displayed on both panels. The contrast of the panels were compared digitally in Adobe Photoshop. To create a given desired contrast, we measured the required voltage and input current for each panel. The larger panel,

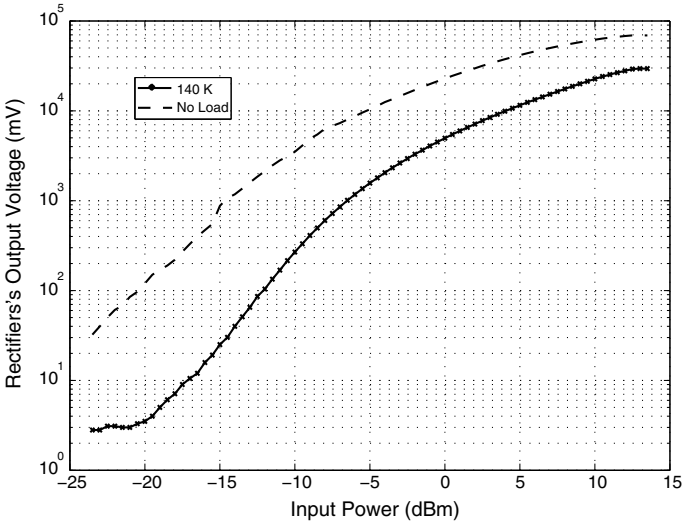

Fig. 18 Performance of the energy-harvester unit

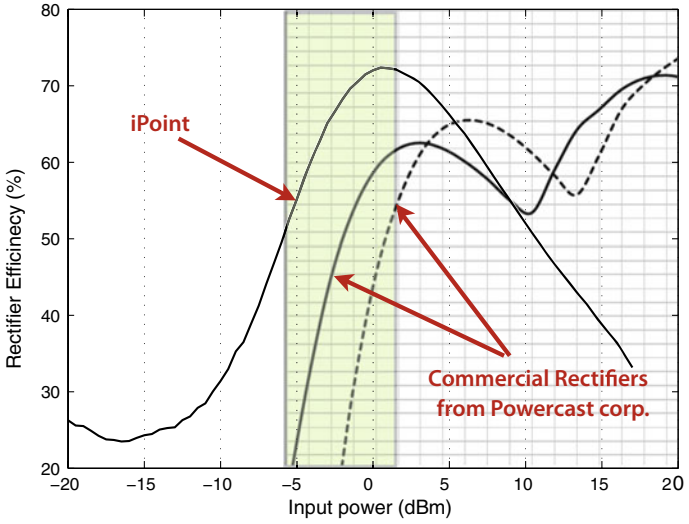

Fig. 19 Energy-harvester efficiency as a function of input power. The shaded region indicates the operating range of the iPoint. Based on our measurements the optimized rectifier in our prototype outperforms state-of-the-art commercial rectifier chips within desired input power range

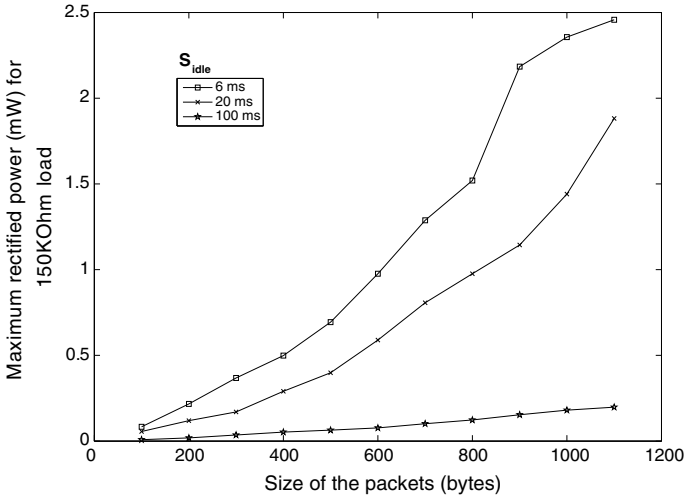

Fig. 20 The rectified output voltage as a function of the packet length for different idle times S_{idle} (therefore duty cycles)

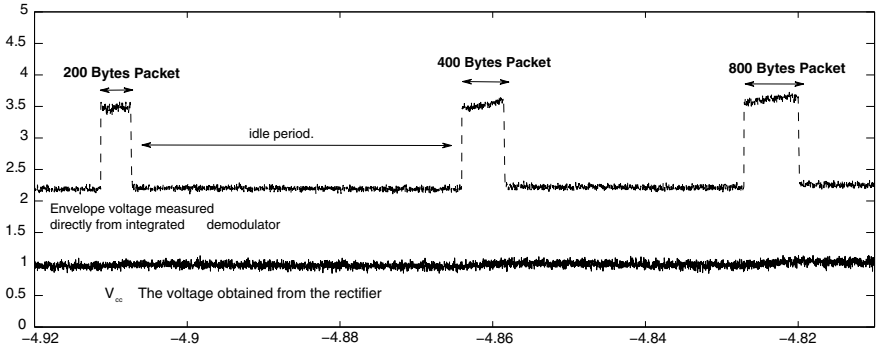

Fig. 21 The voltage of energy harvester V_{cc} and integrated demodulator (envelope signal) in Volts. Note that, the size of the packet is easily detectable. The Wi-Fi communication rate was fixed to 1 Mbps. harvester's output level is fairly smaller than the peaks of envelope signal. That reason is the long idle times between packet transmissions. The data is captured by a Infinium MSO8104 oscilloscope from Agilent Technologies. The plot is regenerated in MATLAB

requires 2.9 V drawing 49 μA (142.1 μW), whereas Panel 2 requires 1.9 V drawing 21 μA (39.9 μW).

PLM Decoding Performance In order to test the functionality of the integrated demodulator of the front end, packets with different sizes were sent over the Wi-Fi channel by the smartphone while the output of the energy harvester and integrated demodulator being measured. The rate of communication was fixed to 1 Mbps. The result is shown in Fig. 21.

4.8 Summary

In this section, we introduced iPoint, a device that can interact with commodity smartphones, equipped with a Wi-Fi network interface and camera, therefore enabling ad hoc and universal communication. The energy and information are exchanged in an instance of a previously described CEICh channel. At the core of iPoint lies an ultra-low-power microcontroller. iPoint draws the entire of its energy from the smartphone transmissions, through an RF energy-harvester, making the use of batteries unnecessary and guaranteeing its longevity. Two new communication paradigms are introduced:

- Packet width modulation allows the smartphone to encode information in the width of the Wi-Fi packet and making demodulation extremely energy-efficient
- LCD information encoding and camera decoding.

We discussed several design possibilities and built a prototype of the iPoint. We reported on the performance of our system for various transmission powers, operation frequencies of the microcontroller, packet sizes and duty cycles.

5 Conclusion and Future Research Directions

Energy efficiency of wireless communications remains a key obstacle that greatly influences the overall performance of wireless networks. Critical dependency of wireless devices on their limited source of energy requires careful adjustments in computations and communication to conserve as much energy as possible. In some particular applications of wireless communication, the energy conservation issue becomes so severe that having a local source of energy (battery) is not practical or feasible. One example of such scenario can be observed in wireless sensor networks in which the sensor node consumes a vast majority of its energy on keeping its wireless radio on waiting for a typically rare incoming message. In this work, we explore the wireless transfer of energy alongside information as a solution to energy conserving problem in the aforementioned scenarios.

We have presented the notion of consolidated energy and information channel for wireless sensor networks. We argue that energy conservation issues at the receiver side can be eliminated by transferring energy via wireless signals. We have reviewed the steps required to enable such functionality in wireless sensor networks, studied potential wireless energy transfer methods, and presented the necessary modifications to wireless communication after the integration of energy transfer. We have introduced iPoint, a passively powered wireless device that is capable of communicating with a commodity smartphone without any need for a battery or any specific hardware modification on the phone. The complete design and optimization of the software and hardware of the device were presented. We presented two new communication schemes: packet length modulation (PLM) and LCD pattern coding (LPC).

We provided the theoretical performance analysis, and also performed a rigorous experimental evaluation of the system. iPoint is an example of a wireless device that consumes no energy unless it is necessary. At first glance, this seems similar to the functionality of RFID passive tags. However, iPoint's ability to communicate with a device as common as a smartphone without any hardware modification (just by installing an application) makes the information much more accessible. The design of the passively powered devices is a vastly complex problem. While we tried to optimize the different components of the design as much as possible, there is still room for improvement. In the future research, it would be interesting to consider more sophisticated antenna designs to improve the energy harvesting performance. Another interesting problem is to study the effects of installing security schemes on top of the presented communication protocols on the overall energy efficiency of the system.

References

1. Adair, R.K.: Constraints on biological effects of weak extremely-low-frequency electromagnetic fields. Phys. Rev. A **43**(2), 1039–1048 (1991)
2. Adair, R.K.: Vibrational resonances in biological systems at microwave frequencies. Biophys J **82**(3), 1147–52 (2002)
3. Alphandéry, E., Faure, S., Raison, L., Duguet, E., Howse, P.A., Bazylinski, D.A.: Heat production by bacterial magnetosomes exposed to an oscillating magnetic field. J. Phys. Chem. C **115**(1), 18–22 (2011)
4. WiTricity Corp. http://www.witricity.com/pages/technology.html
5. Del Barco, E., Asenjo, J., Zhang, X., Pieczynski, R., Julia, A., Tejada, J., Ziolo, R.F., Fiorani, D., Testa, A.M.: Free rotation of magnetic nanoparticles in a solid matrix. Chem. Mater. **13**(5), 1487–1490 (2001)
6. Bennett, C.: Logical reversibility of computation. IBM J. Res. Dev. **17**(6), 525–536 (1973)
7. Berridge, M.:The AM and FM of calcium signalling. Nature (1997)
8. Blakemore, R.: Magnetotactic bacteria. Science **190**(4212), 377–379 (1975)
9. Buettner, M., Prasad, R., Sample, A., Yeager, D., Greenstein, B., Smith, J.R., Wetherall, D.: Rfid Sensor Networks with the Intel Wisp. pp. 393–394 (2008)
10. Blatt, J.M., Weisskopf, V.F.: Theoretical Nuclear Physics, p. 864 (1954)
11. Chen, C.: Remote control of living cells. Nature Nanotechnology (2008)
12. Cifra, M.: Electrodynamic eigenmodes in cellular morphology. BioSystems **109**(3), 356–66 (2012)
13. Cohen, R., Kapchits, B.: An optimal wake-up scheduling algorithm for minimizing energy consumption while limiting maximum delay in a mesh sensor network. IEEE/ACM Trans. Netw. **17**(2), 570–581 (2009)
14. Chaubey, A., Malhotra, B.D.: Mediated biosensors. Biosens. Bioelectron. **17**(6–7), 441–456 (2002)
15. Choi, J.H., Nguyen, F.T., Barone, P.W., Heller, D.A., Moll, A.E., Patel, D., Boppart, S.A., Strano, M.S.: Multimodal biomedical imaging with asymmetric single-walled carbon nanotube/iron oxide nanoparticle complexes. Nano Lett. **7**(4), 861–867 (2007). Apr
16. Cockcroft, J.D., Walton, E.T.S.: Experiments with high velocity positive ions. (i) further developments in the method of obtaining high velocity positive ions. Proc. R Soc. Lond. Ser. A **136**(830), 619–630 (1932)

17. Correia, L.M., Zeller, D., Blume, O., Ferling, D., Jading, Y., Góanddor, I., Auer, G., Van Der Perre, L.: Challenges and enabling technologies for energy aware mobile radio networks. IEEE Commun. Mag. **48**(11):66–72 (2010)
18. Dykman, M.I., Khasin, M., Portman, J., Shaw, S.W.: Spectrum of an oscillator with jumping frequency and the interference of partial susceptibilities. Phys. Rev. Lett. **105**(23), 230601 (2010)
19. Dobson, J.: Remote control of cellular behaviour with magnetic nanoparticles. Nat. Nanotechnol. (2008)
20. Degen, C.L., Poggio, M., Mamin, H.J., Rettner, C.T., Rugar, D.: Nanoscale magnetic resonance imaging. Proc. Natl. Acad Sci. USA **106**(5), 1313–1317 (2009)
21. Drubach, D.: The Brain Explained, p. 168, Jan 2000
22. Ermolov, V., Heino, M., Karkkainen, A., Lehtiniemi, R., Nefedov, N., Pasanen, P., Radivojevic, Z., Rouvala, M., Ryhanen, T., Seppala, E., Uusitalo, M.: Significance of nanotechnology for future wireless devices and communications. In: 2007 IEEE 18th International Symposium on Personal, Indoor and Mobile Radio Communications, PIMRC 2007, pp. 1–5 (2007)
23. EPCglobal Standards and Technology. http://www.epcglobalinc.org/standards (2008)
24. Falas, T., Kashani, H.: Two-dimensional Bar-code Decoding With Camera-equipped Mobile Phones, pp. 597–600, Mar 2007
25. Glogauer, M., Ferrier, J., McCulloch, C.A.: Magnetic fields applied to collagen-coated ferric oxide beads induce stretch-activated ca2+ flux in fibroblasts. Am. J. Physiol. **269**(5 Pt 1), C1093–104 (1995)
26. Havelka, D., Cifra, M., Kučera, O., Pokorný, J., Vrba, J.: High-frequency electric field and radiation characteristics of cellular microtubule network. J. Theor. Biol. **286**(1), 31–40 (2011)
27. Hu, X., Cebe, P., Weiss, A.S., Omenetto, F., Kaplan, D.L.: Protein-based composite materials. Mat. Today **15**(5), 208–215 (2012)
28. Hergt, R., Dutz, S., Müller, R., Zeisberger, M.: Magnetic particle hyperthermia: nanoparticle magnetism and materials development for cancer therapy. J. Phys. Condens. Matter **18**, S2919 (2006)
29. Huang, H., Delikanli, S., Zeng, H., Ferkey, D.M., Pralle, A.: Remote control of ion channels and neurons through magnetic-field heating of nanoparticles. Nat. Nanotechno. **5**(8), 602–606 (2010)
30. Howard, J., Hudspeth, A.J.: Compliance of the hair bundle associated with gating of mechanoelectrical transduction channels in the bullfrog's saccular hair cell. Neuron **1**(3), 189–99 (1988)
31. Hughes, S., El Haj, A.J., Dobson, J.: Magnetic micro- and nanoparticle mediated activation of mechanosensitive ion channels. Med. Eng. Phys. **27**(9), 754–62 (2005)
32. Hamam, R.E., Karalis, A., Joannopoulos, J.D., Soljačić, M.: Coupled-mode theory for general free-space resonant scattering of waves. Phys. Rev. A **75**(5), 53801 (2007)
33. Hughes, S., McBain, S., Dobson, J., El Haj, A.J.: Selective activation of mechanosensitive ion channels using magnetic particles. J. R. Soc. Interface **5**(25), 855–63 (2008)
34. Iyer, V., Talla, V., Kellogg, B., Gollakota, S., Smith, J.: Inter-technology backscatter: towards internet connectivity for implanted devices. In: Proceedings of the 2016 ACM SIGCOMM Conference (SIGCOMM '16), pp. 356–369. ACM, New York, NY, USA
35. HTC dream (T-mobile g1). http://www.htc.com/www/product/dream/overview.html
36. Jackson, J.D.: Classical Electrodynamics (1967)
37. Javaheri, H.: Wireless Transfer of Energy Alongside Information: From Wireless Sensor Networks to Bio-Enabled Wireless Networks. Ph.D. Dissertation. Northeastern Univ., Boston, MA, USA, Dec 2012
38. Javaheri, H., Barbiellini, B., Noubir, G.: Efficient magnetic torque transduction in biological environments using tunable nanomechanical resonators. In: 2011 Proceedings of the IEEE EMBC (2011)
39. Javaheri, H., Barbiellini, B., Noubir, G.: Efficient magnetic torque transduction in biological environments using tunable nanomechanical resonators. Conf. Proc. IEEE Eng. Med. Biol. Soc. **2011**, 1863–6 (2011)

40. Javaheri, H., Barbiellini, B., Noubir, G.: On the energy transfer performance of mechanical nanoresonators coupled with electromagnetic fields. cond-mat.mes-hall, Aug 2011
41. Javaheri, H., Barbiellini, B., Noubir, G.: On the energy transfer performance of mechanical nanoresonators coupled with electromagnetic fields. Nanoscale Res. Lett. **7**(1), 572 (2012)
42. Javaheri, H., Noubir, G.: ipoint: A platform-independent passive information kiosk for cell phones. In: 2010 7th Annual IEEE Communications Society Conference onSensor Mesh and Ad Hoc Communications and Networks (SECON), pp. 1–9 (2010)
43. Javaheri, H., Noubir, G., Noubir, S.: Rf control of biological systems: Applications to wireless sensor networks. Nano-Net (2009)
44. Janssen, X.J.A., Schellekens, A.J., van Ommering, K., van IJzendoorn, L.J., Prins, M.W.J.: Controlled torque on superparamagnetic beads for functional biosensors. Biosens. Bioelectron. **24**(7), 1937–1941 (2009)
45. Jensen, K., Weldon, J., Garcia, H., Zettl, A.: Nanotube radio. Nano letters **7**(11), 3508–3511 (2007)
46. Kirschvink, J.L.: Comment on constraints on biological effects of weak extremely-low-frequency electromagnetic fields. Phys. Rev. A (1992)
47. Karalis, A., Joannopoulos, J.D., Soljacic, M.: Efficient wireless non-radiative mid-range energy transfer. Ann. Phys. **323**(1), 34–48 (2008)
48. Kobayashi, A., Kirschvink, J.L.: Magnetoreception and electromagnetic field effects: sensory perception of the geomagnetic field in animals and humans. ACS Adv. Chem. Ser. **250**, 367–394 (1995)
49. Kirschvink, J.L., Kobayashi-Kirschvink, A., Diaz-Ricci, J.C., Kirschvink, S.J.: Magnetite in human tissues: a mechanism for the biological effects of weak elf magnetic fields. Bioelectromagn. Suppl **1**, 101–13 (1992)
50. Kurs, A., Karalis, A., Moffatt, R., Joannopoulos, J.D., Fisher, P., Soljacic, M.: Wireless power transfer via strongly coupled magnetic resonances. Science **317**(5834), 83 (2007)
51. Kim, D.H., Rozhkova, E.A., Ulasov, I.V., Bader, S.D., Rajh, T., Lesniak, M.S., Novosad, V.: Biofunctionalized magnetic-vortex microdiscs for targeted cancer-cell destruction. Nat. Mater. (2009)
52. Kirschvink, J.L., Winklhofer, M., Walker, M.M.: Biophysics of magnetic orientation: strengthening the interface between theory and experimental design. J. R. Soc. Interface **7**, S179–S191 (2010). Jan
53. Le, T., Mayaram, K., Fiez, T.: Efficient far-field radio frequency energy harvesting for passively powered sensor networks. IEEE J. Solid-State Circuits **43**(5), 1287–1302 (2008)
54. Lahiri, I., Oh, S., Hwang, J.Y., Cho, S., Sun, Y., Banerjee, R., Choi, W.: High capacity and excellent stability of lithium ion battery anode using interface-controlled binder-free multiwall carbon nanotubes grown on copper. ACS Nano **4**(6), 3440–3446 (2010)
55. Malcolm, R.: A mechanism by which the hair cells of the inner ear transduce mechanical energy into a modulated train of action potentials. J. Gen. Physiol. **63**(6), 757 (1974)
56. Meyer, C.J., Alenghat, F.J., Rim, P., Fong, J.H., Fabry, B., Ingber, D.E.: Mechanical control of cyclic amp signalling and gene transcription through integrins. Nat. Cell Biol. **2**(9), 666–8 (2000)
57. Meirovitch, L.: Fundamentals of Vibrations (2001)
58. McSpadden, J.O., Mankins, J.C.: Space solar power programs and microwave wireless power transmission technology. IEEE Microw. Mag. **3**(4), 46–57 (2002)
59. Muxworthy, A.R., Williams, W.: Critical superparamagnetic/single-domain grain sizes in interacting magnetite particles: implications for magnetosome crystals. J. R. Soc. Interface **6**(41), 1207–12 (2009)
60. Mohan, A., Woo, G., Hiura, S., Smithwick, Q., Raskar, R.: Bokode: imperceptible visual tags for camera based interaction from a distance. ACM Trans. Graph. **28**(3):98:1–98:8 (2009)
61. Mishra, D., De, S., Jana, S., Basagni, S., Chowdhury, K., Heinzelman, W.: Smart RF energy harvesting communications: challenges and opportunities. IEEE Commun. Mag. **53**(4), 70–78 (2015)
62. The Near Field Communication Forum. http://www.nfc-forum.org/

63. Nelson, P.C., Radosavljević, M., Bromberg, S.: Biological Physics: Energy, Information, Life, p. 630, Jan 2008
64. Nakano, T., Suda, T., Koujin, T., Haraguchi, T., Hiraoka, Y.: Molecular communication through gap junction channels. Trans. Comput. Syst. Biol. X (2008)
65. Nakano, T., Suda, T., Moore, M., Egashira, R., Enomoto, A., Arima, K.: Molecular communication for nanomachines using intercellular calcium signaling. In: 2005 5th IEEE Conference on Nanotechnology, pp. 478– 481, vol. 2 (2005)
66. Phizicky, E.M., Fields, S.: Protein-protein interactions: methods for detection and analysis. Microbiol. Rev. **59**(1), 94–123 (1995)
67. Poon, A., O'Driscoll, S., Meng, T.: Optimal frequency for wireless power transmission into dispersive tissue. IEEE Trans. Antennas Propag. **58**(5), 1739–1750 (2010)
68. Poon, A.S.Y.: Miniaturization of implantable wireless power receiver. Conf. Proc. IEEE Eng. Med. Biol. Soc. **2009**, 3217–20 (2009)
69. PowerCast Corporation. http://www.powercastco.com/technology/powerharvester-receivers
70. Proakis, J.G., Salehi, M.: Digital Communications (2008)
71. Rabaey, J.: Wireless beyond the third generation-facing the energy challenge. In: Low Power Electronics and Design, Jan 2002
72. Rice, S.O.: Mathematical Analysis of Random Noise
73. RamRakhyani, A.K., Lazzi, G.: On the design of efficient multi-coil telemetry system for biomedical implants. IEEE Trans. Biomed. Circuits Syst. **PP**(99), 1 (2012)
74. Raghunathan, V., Schurgers, C., Park, S., Srivastava, M.B.: Energy-aware wireless microsensor networks. IEEE Signal Process. Mag. **19**(2), 40–50 (2002)
75. Sazonova, V.A.: A Tunable Carbon Nanotube Resonator (2006)
76. Soloveichik, D., Cook, M., Winfree, E., Bruck, J.: Computation with finite stochastic chemical reaction networks. Nat. Comput. Int. J. **7**(4) (2008)
77. Shetty, R.P., Endy, D., Knight, T.F.: Engineering biobrick vectors from biobrick parts. J. Biol. Eng. **2**, 5 (2008)
78. Sidles, J.A.: Spin microscopy's heritage, achievements, and prospects. Proc. Nat. Acad. Sci. USA **106**(8), 2477–8 (2009)
79. Stipe, B., Mamin, H., Stowe, T., Kenny, T., Rugar, D.: Magnetic dissipation and fluctuations in individual nanomagnets measured by ultrasensitive cantilever magnetometry. Phys. Rev. Lett. **86**(13), 2874–2877 (2001)
80. Shah, R.C., Rabaey, J.M.: Energy Aware Routing for Low Energy Ad Hoc Sensor Networks, vol. 1, pp. 350–355, Mar 2002
81. Schurgers, C., Raghunathan, V., Srivastava, M.B.: Power management for energy-aware communication systems. ACM Trans. Embed. Comput. Syst. **2**(3), 431–447 (2003)
82. Samanta, B., Yan, H., Fischer, N.O., Shi, J., Jerry, D.J., Rotello, V.M.: Protein-passivated fe3o4 nanoparticles: low toxicity and rapid heating for thermal therapy. J. Mater. Chem. **18**(11), 1204 (2008)
83. Sample, A.P., Yeager, D.J., Powledge, P.S., Mamishev, A.V., Smith, J.R.: Design of an rfid-based battery-free programmable sensing platform. IEEE Trans. Instrum. Measur. **57**(11), 2608–2615 (2008)
84. Takata, H., Kogure, O., Murase, K.: Matrix-addressed Liquid Crystal Displays, vol. 18, pp. 72 (1972)
85. Tanaka, K., Kenichiro, M., Takahashi, M., Ishii, T., Sasaki, S.: Development of bread board model for microwave power transmission experiment from space to ground using small scientific satellite. pp. 191–194, May 2012
86. Visser, H.J., Reniers, A.C.F., Theeuwes, J.A.C.: Ambient rf Energy Scavenging: Gsm and Wlan Power Density Measurements, pp. 721–724, Oct 2008
87. Wang, J.: Carbon-nanotube based electrochemical biosensors: a review. Electroanalysis (2005)
88. Weinstein, R.: RFID: a technical overview and its application to the enterprise. IT Prof. **7**(3), 27–33 (2005)
89. Winklhofer, M., Kirschvink, J.L.: A quantitative assessment of torque-transducer models for magnetoreception. J. R. Soc. Interface **7**, S273–S289 (2010)

90. Weiss, B.P., Kim, S.S., Kirschvink, J.L., Kopp, R.E., Sankaran, M., Kobayashi, A., Komeili, A.: Magnetic tests for magnetosome chains in martian meteorite alh84001. Proc. Nat. Acad. Sci. USA **101**(22), 8281–8284 (2004)
91. Wendt, T.M., Reindl, L.M.: Wake-Up Methods to Extend Battery Life Time of Wireless Sensor Nodes, pp. 1407–1412, May 2008
92. Yaghjian, A.: An overview of near-field antenna measurements. IEEE Trans. Antennas Propag. (1986)
93. Yoo, T.-W., Chang, K.: Theoretical and experimental development of 10 and 35 ghz rectennas. IEEE Trans. Microw. Theory Tech. **40**(6), 1259–1266 (1992)
94. Zahradka, K., Slade, D., Bailone, A., Sommer, S., Averbeck, D., Petranovic, M., Lindner, A.B., Radman, M.: Reassembly of shattered chromosomes in deinococcus radiodurans. Nature **443**(7111), 569–573 (2006)